R. & M. No. 3683






MINISTRY OF DEFENCE
AERONAUTICAL RESEARCH COUNCIL
REPORTS AND MEMORANDA

# TWO-DIMENSIONAL SELF-PRESERVING TURBULENT MIXING LAYERS AT DIFFERENT FREE STREAM VELOCITY RATIOS

By A. J. YULE
Department of the Mechanics of Fluids,
University of Manchester

LONDON: HER MAJESTY'S STATIONERY OFFICE
1972
PRICE £1·38 NET

# TWO-DIMENSIONAL SELF-PRESERVING TURBULENT MIXING LAYERS AT DIFFERENT FREE STREAM VELOCITY RATIOS

By A. J. YULE
Department of the Mechanics of Fluids,
University of Manchester



*Reports and Memoranda No.* 3683*
*March*, 1971

*Summary*
Turbulence and mean velocity measurements have been made in two mixing layers with free stream velocity ratios of 0·30 and 0·61 and these measurements are compared with the classical free mixing layer investigation of Liepmann and Laufer. The experiments indicate changes in the intensity levels and the structure of the turbulence with changing free stream velocity ratio.

LIST OF CONTENTS

*Section*



*Replaces A.R.C. 32 732.

---

1. *Introduction*

There is little experimental data on the mixing of two non-zero velocity airstreams and published experimental results are often contradictory and of doubtful accuracy. Extensive turbulence measurements exist for the case of a free mixing layer only. Knowledge of how the structure of a mixing layer is modified by the presence of a secondary stream is of great practical importance particularly in connection with the problem of jet noise. Previous experimenters have found that most of the exhaust noise of a free jet is produced within the first fifteen nozzle diameters of the jet where a mixing layer type of flow is dominant. The presence of a secondary stream is relevant to an aircraft in flight and to the ducted jet or ejector type of flow.

Experimenters have made a bare minimum of measurements in a comparatively large number of mixing layers with different free stream velocity ratios. Their measurements were almost entirely restricted to mean velocity distributions and consequently the effects of the turbulence in the separating plate boundary layers, in the free streams and in the boundary layers on the walls of the channel restricting the flow were neglected. Because of this the results of these experiments show a remarkable disagreement between each other and with a few exceptions they are of use only in showing the sensitivity of a mixing layer to deviations from ideal conditions.

The present worker recognised the importance of turbulence measurements in mixing layers not only for discovering whether (and where) the assumed ideal flow conditions existed but also as a means of discovering how the basic structure of a mixing layer adapted itself to the presence of a secondary stream. Only two free stream velocity ratios were used for the present experimental investigation but detailed turbulence measurements were made in each of the mixing layers and particular attention was paid to the accuracy of the measurements and to the accuracy of the flows as representations of the ideal self-preserving flows.

2. *Summary of Previous Work.*

It may be deduced from the momentum equation that a mixing layer between two constant velocity incompressible free streams can be self-preserving with a constant rate of increase in thickness (see for example Hinze[1]). Simple dimensional analysis shows that for a self-preserving mixing layer the rate of spread is some function of the free stream velocity ratio $U_2/U_1$ only (see Fig. 1).

Tollmien[2] obtained an analytical solution for the self-preserving mean velocity profile of a mixing layer with one stream at rest (i.e. $U_2 = 0$, the free mixing layer). The boundary layer approximation of the turbulent momentum equation was solved by applying Prandtl's mixing length hypothesis for the turbu-

lent shear stress. Kuethe[3] extended Tollmien's approach to the general case of two non-zero velocity streams. The solutions required the evaluation of an empirical constant which was related to the spreading rate and thus dependent upon $U_2/U_1$. In addition to the two boundary conditions which fixed the mean velocity as $U_1$ and $U_2$ at the inner and outer edges of the mixing layer respectively, a third boundary condition was needed which effectively fixed the lateral position of the mixing layer relative to the co-ordinate system. Kuethe considered the flow produced by the mixing of two semi-infinite, initially parallel free streams, the $Ox$ axis being parallel to the initial directions of the streams (see Fig. 1). For such a flow the mixing layer produces deviations in the mean streamlines of the free streams in a similar fashion to those occurring in the free stream of a boundary layer flow. However, the absence of a solid surface makes it impossible to use a simple third boundary condition (such as $V = 0$ at $Y = 0$ for the boundary layer) and Kuethe used a qualitative third boundary condition which was suggested by von Karman i.e.

$$U_1 V_1 + U_2 V_2 = 0 \tag{1}$$

Kuethe's analysis produced a relatively simple equation for the mean velocity distribution but it suffered from discontinuities in the velocity gradients at the edges of the mixing layer.

Görtler[4] solved the same problem as Kuethe by using Prandtl's second hypothesis for the turbulent shear stress, (i.e. the constant eddy viscosity hypothesis). No attempt was made at fixing the lateral position of the solution by using a third boundary condition. Görtler's solution, though more complex than that of Kuethe, was later found to give very good agreement with the shape of experimental velocity profiles and the solution, or an approximation to it, is very often used in mixing layer investigations. Like Kuethe the solution required the empirical knowledge of a parameter, $\sigma$, related to the rate of spread of the mixing layer, $d\delta/dx$, and thus to the free stream velocity ratio, $U_2/U_1$. The constant eddy viscosity analysis is considered in sections 4 and 5.

Liepmann and Laufer[5] made an investigation with hot wire equipment in the free mixing layer formed at the boundary of a half-jet issuing into the ambient atmosphere. Their mean velocity and turbulence measurements indicated that the mixing layer quickly became self-preserving and with suitable choices of the respective empirical constants the solutions of Tollmien and Görtler agreed well with the measured self-preserving mean velocity distribution, with the constant eddy viscosity solution having slightly better accuracy. Several other workers have investigated free mixing layers by using mean velocity measurements only and the results were generally in agreement with those of Liepmann and Laufer (e.g. Albertson[6] et al). The experiment of Liepmann and Laufer remains the most reliable and extensive investigation of a self-preserving mixing layer.

Ting[7] used a method of matched asymptotic expansions to demonstrate that the third boundary condition of von Karman equation (1) was valid in the laminar case and implied that it could be used as a first approximation in the turbulent case. Mills[8] and also Baker and Weinstein[9] used this third boundary condition in their numerical solutions for the mean velocity distributions in mixing layers and they used the same constant eddy viscosity assumption as that made by Görtler. The analytical mean velocity profiles derived for mixing layers at different mean velocity ratios by Mills, Baker and Weinstein and Görtler are in agreement with each other.

Both Baker and Weinstein[10] and Mills performed experiments with mixing layers with several different free stream velocity ratios. Mills investigated two adjacent half jets exhausting into the atmosphere and Baker and Weinstein's mixing layers were produced by two streams mixing in a constant area duct. By suitable choices of the empirical constant related to the spreading rates of the mixing layers the mean velocity distributions in the mixing layers were found to agree well with the constant eddy viscosity solutions. However the absence of any extensive turbulence measurements in their experiments made it impossible to prove that the mixing layers were truly self-preserving and measurements of $\overline{u^2}$ made by Baker and Weinstein appear to indicate rather thick boundary layers on the walls of the duct and on the separating plate and a lack of self-preservation in the mixing layers. As will be shown later there was little correlation between the spreading rates measured by these workers at different velocity ratios.

Experiments upon two stream mixing by Zhestkov et al (unpublished) and Yakovlevskiy[11] were

reported by Abramovich[12]. Abramovich superimposed the velocity measurements of these experimenters for several velocity ratios and he concluded that there was no change in the shape of the self-preserving mean velocity profile with the velocity ratio. However the measurements of Mills and Baker and Weinstein do show changes in the shapes of the velocity profiles the most noticeable being a more rapid approach to the value of the lower velocity stream as $U_2/U_1$ increases. This change in shape is also predicted by the constant eddy viscosity analysis. Abramovich applied dimensional assumptions regarding the lateral diffusion of the turbulence and deduced the following expression for the variation of the spreading rate with the velocity ratio

$$\frac{d\delta}{dx} = \text{constant} \times \frac{1-\dfrac{U_2}{U_1}}{1+\dfrac{U_2}{U_1}} \tag{2}$$

where $\delta$ is the mixing layer width. Abramovich stated that the results of Zhestkov et al and Yakovlevskiy agreed with equation (2) for $U_2/U_1 \leqslant 0{\cdot}4$. Sabin[13] investigated two stream mixing with a water channel. The velocity profiles are lacking in experimental points and only two traversing stations were used for each velocity ratio.

Miles and Shih[14] demonstrated the very wide scatter in the spreading rates measured by Sabin, Zhestkov et al and Yakovlevskiy and they proposed that this scatter was caused by the persistence of separating plate boundary layer effects in the mixing layers. They performed experiments with apparatus of the open jet type in which separating plate boundary layers were removed by suction and they found a smooth variation in the spreading rate with changing velocity ratio. No turbulence measurements were made but their experimental results must be regarded as the most reliable to date for mixing layers with non-zero velocity secondary streams.

Wygnanski and Fiedler[15] investigated a free mixing layer and they made extensive measurements of the turbulence components in a similar investigation to that of Liepmann and Laufer. However their turbulence levels and rate of spread differed significantly from those measured by Liepmann and Laufer. This discrepancy is discussed by Yule[16].

3. *Basic Equations and Coordinate System.*

Instead of the flow proposed by Kuethe and other investigators which assumed the mixing of two initially parallel free streams an ideal self-preserving flow is assumed here. It can be shown from the equations of motion that a mixing layer can only be self-preserving if the free streams have constant velocity components $U_1$, $V_1$, $U_2$ and $V_2$ at the edges of the mixing layer. As can be seen from Fig. 1 this requires pressure gradients in the flow considered by Kuethe et al but pressure gradients are not strictly compatible with the requirements of self-preservation. The ideal self-preserving flow proposed here assumes that the free streams have uniform and constant velocities outside the mixing layer but their directions differ due to the entrainment action of the mixing layer (see Fig. 2). The $Ox$ axis is chosen to be in the direction of the higher velocity stream so that there is the exact third boundary condition, $V_1 = 0$, and not the approximate third boundary condition equation (1) involved in Kuethe's flow. The origin of the coordinate system is at the virtual origin of the mixing layer.

For a mixing layer with no longitudinal static pressure gradients in the free streams the longitudinal equation of motion is (see Townsend[17])

$$U\frac{\partial U}{\partial x} + V\frac{\partial U}{\partial y} + \frac{\partial \overline{uv}}{\partial y} = 0 \tag{3}$$

The experiments of Liepmann and Laufer and those of the present author show that the normal stress term and the viscous term in Townsend's equation (equation (8.3.3)) are at least third order and can be neglected for the present purposes.

The condition for incompressibility is,

$$\frac{\partial U}{\partial x}+\frac{\partial V}{\partial y}=0. \tag{4}$$

A similarity variable $\eta=\dfrac{y}{x}$ is defined with self-preserving functions $\bar{f}(\eta)$ and $\bar{g}(\eta)$ so that $U=U_2+(U_1-U_2)\bar{f}(\eta)$, and $\overline{uv}=(U_1-U_2)^2\,\bar{g}(\eta)$. Note that $\bar{f}$ and $\bar{g}$ are also dependent upon the velocity ratio $U_2/U_1$.

The self-preserving form of equation (3), substituting for $V$ from equation (4) is

$$\frac{U_1}{U_1-U_2}\eta\bar{f}'+\bar{f}'\int_{-\infty}^{\eta}(\bar{f}-1)\,d\eta-\bar{g}=0, \tag{5}$$

with $V=0$ at $y=-\infty$.

Integrating equation (5) with respect to $\eta$ from $\eta=-\infty$ to an arbitrary value yields,

$$\bar{g}=\frac{U_1}{U_1-U_2}\left\{\eta(\bar{f}-1)-\int_{-\infty}^{\eta}(\bar{f}-1)d\eta\right\}+(\bar{f}-1)\int_{-\infty}^{\eta}(\bar{f}-1)d\eta-\int_{-\infty}^{\eta}(\bar{f}-1)^2d\eta.$$

If the mean velocity distribution in a self-preserving mixing layer is known accurately equation (6) can give the turbulent shear-stress distribution.

The value of the transverse velocity component in the lower velocity stream may be found by integrating the self-preserving form of equation (4) to give

$$V_2=(U_1-U_2)\int_{-\infty}^{+\infty}\bar{f}'\,\eta\,d\eta. \tag{7}$$

The angle $\alpha$ between the two streams is thus (*see* Fig. 2)

$$\alpha=\tan^{-1}\left(-\frac{V_2}{U_2}\right)=\tan^{-1}\left\{\frac{U_2-U_1}{U_2}\int_{-\infty}^{+\infty}\bar{f}'\,\eta\,d\eta\right\}. \tag{8}$$

It is necessary to find the position of the $Ox$ axis when the shape of the mean velocity distribution is known. This is most easily achieved by assuming definite values for the edges of the mixing layer $\eta_1$ and $\eta_2$ such that $\eta=\eta_2$ at $\bar{f}=0$ and $\eta=\eta_1$ at $\bar{f}=1$. Equation (5) is integrated across the mixing layer to give,

$$\eta_1=-\frac{U_1-U_2}{U_1}\left\{\int_{\eta_1}^{\eta_2}\bar{f}^2\,d\eta+\frac{U_2}{U_1-U_2}\int_{\eta_1}^{\eta_2}\bar{f}\,d\eta\right\} \tag{9}$$

Only the shape of the function $\bar{f}$ is needed to evaluate $\eta_1$ and hence $\eta_2$ from equation (9).

4. *The Constant Eddy Viscosity Solution.*

Görtler[4] assumed the eddy viscosity, $\nu_T$, to be constant across any section of a mixing layer and he used Prandtl's second hypothesis to write,

$$\nu_T = K_G \delta (U_1 - U_2) \tag{10}$$

where $K_G$ is a universal constant and $\nu_T = -\dfrac{\overline{uv}}{\dfrac{\partial \overline{U}}{\partial y}}$. Görtler wrote equation (3) in terms of a non-dimensional self-preserving stream function $F(\zeta)$, where $\zeta = \dfrac{\sigma y}{x}$ and

$$\psi = \tfrac{1}{2} x (U_1 + U_2) F(\zeta) \tag{11}$$

He obtained the following equation,

$$F''' + 2\sigma F F'' = 0, \tag{12}$$

where the similarity parameter, $\sigma$, was defined as

$$\sigma = \tfrac{1}{2} \left\{ K_G \frac{d\delta}{dx} \frac{U_1 - U_2}{U_1 + U_2} \right\}^{-\frac{1}{2}}. \tag{13}$$

The boundary conditions of equation (12) are $F' = 1 \pm \dfrac{U_1 - U_2}{U_1 + U_2}$ at $\zeta = \pm \infty$. Görtler solved equation (12) as a power series expansion of the form

$$\sigma F(\zeta) = F_0(\zeta) + \left(\frac{U_1 - U_2}{U_1 + U_2}\right) F_1(\zeta) + \left(\frac{U_1 - U_2}{U_1 + U_2}\right)^2 F_2(\zeta) + \ldots . \tag{14}$$

The first two terms of Görtler's solution in terms of the mean velocity distribution are,

$$U = \frac{U_1 + U_2}{2} \left( 1 + \frac{U_1 - U_2}{U_1 + U_2} \operatorname{erf} \zeta \right). \tag{15}$$

It is seen that Görtler arbitrarily selected an $Ox$ axis direction so that $U = (U_1 + U_2)/2$ at $\zeta = 0$ in his first order solution. Ting[7], Mills[8] and other workers recognised the need for a third boundary condition to fix the lateral position of the solution (i.e. if $F(\zeta)$ is a solution then $F(\zeta + \text{any constant})$ is also a solution if only two boundary conditions are known). Mills and Baker and Weinstein solved equation (12) numerically and used equation (1) as a third boundary condition. In the ideal self-preserving flow which is assumed here the solutions of Mills, Baker and Weinstein and Görtler for the $U$-velocity distribution are applicable but the lateral position of the solution is fixed by the third boundary condition $V = 0$ at $y = -\infty$ which is most easily applied by using equation (9).

5. *The Constant Eddy Viscosity Hypothesis and the Spreading Rates of Mixing Layers.*

The self-preserving form of the mean velocity in terms of Görtler's similarity variable $\zeta$ is $U = U_2 + (U_1 - U_2) f(\zeta)$.

Görtler's eddy viscosity analysis is incomplete in that it provides no relation for the similarity parameter $\sigma$ in terms of the mean velocity ratio $U_2/U_1$. However Yule[16] demonstrated that the constant eddy viscosity hypothesis does imply an analytical relationship for $\sigma$ without the use of further assumptions. It is found that

$$\sigma = \frac{1}{4 K_G A} \frac{U_1 + U_2}{U_1 - U_2} = \sigma_o \frac{1 + U_2/U_1}{1 - U_2/U_1} \tag{16}$$

and

$$\frac{db}{dx} = A \sigma^{-1} \tag{17}$$

where $b$ is the local mixing layer length scale, $A$ is a constant and $\sigma_o$ isht e value of $\sigma$ at $U_2/U_1 = 0$. Equation (16) is also implied by Abramovich's relation for the spreading rate equation (2). As was shown by Miles and Shih[14] and Yule[16] equation (16) is not in agreement with experimental results.

Yule[16] showed that a more logical form of the eddy viscosity hypothesis was obtained when the eddy viscosity was based upon the energy containing turbulence in the mixing layer and the following equation was derived

$$\sigma = \frac{1}{4K_Y A}\left(\frac{(\overline{q^2}_{\max})^{\frac{1}{2}}}{(U_1 - U_2)}\right)^{-1}\frac{U_1 + U_2}{U_1 - U_2}, \tag{18}$$

where $K_Y$ is a constant. It is seen that if the turbulence structure of a mixing layer is the same for all values of $U_2, U_1$ so that $(q^2_{\max})^{\frac{1}{2}} \propto (U_1 - U_2)$ as was implicitly assumed by Abramovich, then equation (18) reduces to equation (16).

6. *Apparatus.*

The mixing layer apparatus (Fig. 3) was installed in the Low Turbulence Tunnel of the Mechanics of Fluids Department's Laboratory at the University of Manchester. Contractions and pressure dropping gauzes were used to produce two streams with steady uniform velocities and equal static pressures. (See Yule[18] for a full description of the apparatus and its design). The dimensions of the working section in which the mixing layers existed were 0·28 m (height), 0·5 m (width) and 1·2 m (length). The trailing edge thickness of the separating plate was 0·3 mm and the trailing edge was 0·14 m above the floor of the working section. This horizontal floor was flat and parallel to the separating plate trailing edge and it was drilled with traversing stations and static pressure tappings at intervals along its complete length. The shape of the roof of the working section was adjusted to achieve the constant longitudinal distributions of static pressure required for self-preservation.

Flow measurements were made with DISA hot wire equipment. Miniature 55A15 probes were used for $U$ and $(\overline{u^2})^{\frac{1}{2}}$ measurements and miniature cross-wire probes were used for $(\overline{v^2})^{\frac{1}{2}}$, $(\overline{w^2})^{\frac{1}{2}}$ and $\overline{uv}$ measurements. The electronic equipment consisted of two 55A01 constant temperature anemometers with two 55D10 linearizers and a 55A06 random signal indicator and correlator. The frequency spectra of the 'u' component of the velocity fluctuations was measured by feeding the output of a hot wire–anemometer linearizer combination to either a Muirhead D-788-A low frequency analyser or a D-888-A high frequency analyser. These instruments had a combined range of 5 cps to 22 Kc/s so that the limiting frequency to which the spectra of the turbulence could be measured accurately was determined by the characteristics of the hot wire—anemometer -linearizer. DISA quote a flat response curve for such a combination for frequencies up to 10 Kc/s.

Lateral spatial correlation coefficients were measured with one hot wire probe holder fixed vertically to the tunnel floor so that the wire recorded the '$u$' component of the fluctuating velocity and another parallel hot wire was traversed in the same vertical plane in the direction of the lower velocity free stream. Longitudinal spatial correlation coefficients were measured by using a fixed wire and a moveable wire downstream. The moveable wire was displaced 2 mm above the horizontal wire and also to one side so that wake effects were minimised.

A traversing apparatus allowed probes to be traversed vertically across the centre of the working section for $0 \leqslant x' \leqslant 1$ m where $(x', y')$ is a coordinate system based upon the geometry of the apparatus (*see* Fig. 3). The position of a probe was known to within $\pm 0{\cdot}05$ mm with the aid of a travelling telescope.

7. *Experimental Results and Discussion.*

7.1. *Basic Measurements.*

Two mixing layers were investigated with velocity ratios $U_2/U_1 = 0{\cdot}30$ and $U_2/U_1 = 0{\cdot}61$ and with $U_1$ the same for each mixing layer at 18 m/s. The measurements in both of the mixing layers consisted of a number of vertical traverses across the complete working section for 0·5 mm $\leqslant x' \leqslant$ 0·9 m from which the distributions of $U$, $(u^2)^{\frac{1}{2}}$, $(v^2)^{\frac{1}{2}}$, $(w^2)^{\frac{1}{2}}$ and $uv$ were derived. Measurements of the lateral spatial correlation

coefficient were made in each of the mixing layers and measurements of the longitudinal spatial correlation coefficient and one-dimensional frequency spectra were made in the mixing layer with $U_2/U_1 = 0{\cdot}61$. All hot wires were calibrated before and after each traverse and if the amount of drift in calibration was greater than 2 per cent the measurements were repeated.

Full measurements are presented for the mixing layer with $U_2/U_1 = 0{\cdot}61$ and the self-preserving distributions of the mean velocity and turbulence components are presented for $U_2/U_1 = 0{\cdot}30$. Figs. 4 to 8 give measurements in the dimensionless forms $\dfrac{U-U_2}{U_1-U_2}$, $(\overline{u^2})^{\frac{1}{2}}/(U_1-U_2)$, $(\overline{v^2})^{\frac{1}{2}}/(U_1-U_2)$, $(\overline{w^2})^{\frac{1}{2}}/(U_1-U_2)$ and $\overline{uv}/(U_1-U_2)^2$ using the dimensionless transverse coordinate $\bar{y}$ where $\bar{y} = (y'-y'_{0\cdot9})/(y'_{0\cdot1}-y'_{0\cdot9})$. Subscripts 0·1 and 0·9 denote values at $(U-U_2)/(U_1-U_2) = 0{\cdot}1$ and 0·9 respectively.

A comparison of the distributions at the different longitudinal positions shows that the mixing layer has a region in which geometric similarity exists for each of the quantities and in this region the mixing layer is self-preserving. For $U_2/U_1 = 0{\cdot}61$ self-preservation applies for traverses with $x' \geqslant 0{\cdot}60$ m and, for $U_2/U_1 = 0{\cdot}30$, for traverses in the range $0{\cdot}20 \text{ m} \leqslant x' \leqslant 0{\cdot}60$ m. For $x' > 0{\cdot}60$ m with $U_2/U_1 = 0{\cdot}30$ the boundary layer on the roof of the wind tunnel began to interact with the mixing layer and for $x' < 0{\cdot}60$ m with $U_2/U_1 = 0{\cdot}61$ and $x' < 0{\cdot}20$ m with $U_2/U_1 = 0{\cdot}30$ the mixing layers are developing from the boundary layers at the end of the separating plate. These boundary layers were fully turbulent and had displacement and momentum thickness ($\delta^*$ and $\delta^{**}$ respectively) as follows: for $U_2/U_1 = 0{\cdot}30$, $\delta_1^* = 1{\cdot}4$ mm, $\delta_1^{**} = 0{\cdot}7$ mm, $\delta_2^* = 1{\cdot}5$ mm, $\delta_2^{**} = 0{\cdot}6$ mm and for $U_2/U_1 = 0{\cdot}61$, $\delta_1^* = 1{\cdot}7$ mm, $\delta_1^{**} = 1{\cdot}1$ mm, $\delta_2^* = 3{\cdot}0$ mm and $\delta_2^{**} = 1{\cdot}8$ mm.

The considerably longer distance required for the mixing layer with $U_2/U_1 = 0{\cdot}61$ to attain self-preservation is explained qualitatively by the higher convection velocities which are present for the turbulence in this mixing layer and also by the larger trough in the velocity distribution at the separating plate edge which must be filled by entrainment. For both mixing layers the $(U-U_2)/(U_1-U_2)$ distributions possess similarity over far larger longitudinal ranges than the ranges for which the turbulence component distributions are similar. Thus the similarity of mean velocity measurements cannot be used as a sole criterion for the assumption that self-preservation exists in a mixing layer. This observation has bearing upon the accuracy of the results of experimenters who relied upon mean velocity measurements alone.

The solid lines in Figs. 4 to 8 are the experimental self-preserving distributions of the dimensionless quantities. The self-preserving distributions corrected for hot wire yaw effects by the method of Davies and Bruun[19] are also shown. In order that experimental and constant eddy viscosity solution velocity distributions can be compared the rates of spread of the experimental mixing layers must be derived. The lateral scale, $y'_{0\cdot1}-y'_{0\cdot9}$ is plotted against $x'$ in Fig. 9 and both mixing layers are seen to possess the linear rates of spread which accompany self-preservation. It is found that $\dfrac{d}{dx'}(y'_{0\cdot1}-y'_{0\cdot9}) = 0{\cdot}095$ for $U_2/U_1 = 0{\cdot}30$ and $\dfrac{d}{dx'}(y'_{0\cdot1}-y'_{0\cdot9}) = 0{\cdot}046$ for $U_2/U_1 = 0{\cdot}61$.

The coordinate system of the experimental mixing layers must be changed to the $(x, y)$ system for self-preserving mixing. The virtual origins of the self-preserving mixing layers (i.e. the origins of the $(x, y)$ coordinate systems) are the same for both velocity ratios, being 40 mm upstream of the separating plate edge and 5 mm vertically below the horizontal plane through the separating plate edge. The directions of the $x$-axes in the self-preserving mixing layers were found by using equation (9).

7.2 *Mean Velocity Distributions.*

Experimental values of $\sigma$ were found by matching the analytical and experimental $f(\zeta)$ distributions (Fig. 10). The analytical distributions of Baker and Weinstein were used. The distributions are matched by choosing $\sigma$ values which equalize the gradients of the analytical and experimental curves at their inflexion points. This is the method used by Miles and Shih and it ensures matching in the central regions of the mixing layers where the constant eddy viscosity assumption is most accurate. It was found that $\sigma = 19$ for $U_2/U_1 = 0{\cdot}30$ and $\sigma = 36$ for $U_2/U_1 = 0{\cdot}61$. The shapes of the analytical and experimental velocity distributions are in excellent agreement apart from some divergence at the edges of the mixing layer with $U_2/U_1 = 0{\cdot}61$. The increasing 'S' type symmetry with increasing velocity ratio which is predicted by the constant eddy viscosity analysis is also evident in the measured distributions.

7.3. *Shear Stress Distributions.*

The shear stress calculated from the measured mean velocity for $U_2/U_1 = 0{\cdot}61$ by using equation (6) is included in Fig. 8 together with the measured values after applying the hot wire correction. Both of these agree reasonably well with the distribution given by the constant eddy viscosity analysis with $\sigma = 36$.

7.4. *Distributions of the Total Turbulence Intensity and its Components.*

Liepmann and Laufer[5] measured $\overline{u^2}$ and $\overline{v^2}$ in a self-preserving free mixing layer and these results are compared with the present measurements in Figs. 11 and 12. The peak intensities of both components are seen to increase with increasing velocity ratio and the positions of the peaks move towards the lower velocity stream relative to the mean velocity distribution. These observations also apply to the present self-preserving distributions of $(\overline{w^2})^{\frac{1}{2}}/(U_1 - U_2)$, in Fig. 7.

Comparing the magnitudes of the different intensity components it is seen that, although the magnitudes of the peaks do not differ by more than 15 per cent in any of the mixing layers, in general $\overline{u^2}_{\max} > \overline{w^2}_{\max} > v^2_{\max}$. This relation is obeyed in experiments in other types of free mixing flow e.g. Bradbury's[20] plane jet.

The self-preserving distributions of the non-dimensionalised total turbulence intensity $\overline{q^2}/(U_1 - U_2)^2$, are calculated from the distributions of the intensity components by summation. $\overline{q^2}$ is calculated from Liepmann and Laufer's data by assuming (following Townsend[17])

$$\overline{q^2} = \tfrac{3}{2}(\overline{u^2} + \overline{v^2}). \tag{19}$$

This relation is obeyed to within 5 per cent of $\overline{q^2}_{\max}$ for the present measurements. Distributions of $\overline{q^2}/(U_1 - U_2)^2$ are given in Fig. 13 using $\eta$ as the variable to demonstrate the differing spreading rates of the mixing layers. The dimensionless peak turbulence intensity is seen to increase by 80 per cent from $U_2/U_1 = 0$ to $U_2/U_1 = 0{\cdot}61$.

7.5. *The Eddy Viscosity Hypothesis in the Light of Experimental Results.*

Fig. 14 shows the wide scatter in the experimental values of $\sigma$. Yule[16] pointed out that the most reliable measurements should be those of Liepmann and Laufer, Miles and Shih, Wyganski and Fiedler and the present results and all these were found to give poor agreement with equation (16) but were well represented by an empirical curve

$$\frac{\sigma}{\sigma_o} = \frac{(1 + U_2/U_1)^{\frac{1}{2}}}{(1 - U_2/U_1)} \tag{20}$$

where $\sigma_o = 11$. By combining equations (20) and (18) Yule[16] showed that the experimental $\sigma$ distribution implied a linear distribution of $q^2_{\max}/(U_1 - U_2)^2$ which gave fair agreement with the experimental values. The observed increase in $\overline{q^2}_{\max}/(U_1 - U_2)^2$ with $U_2/U_1$ is connected with changes in the structure of the turbulence with changing velocity ratio and these changes are best observed by examining the spatial correlation and frequency spectra of the turbulence.

7.6. *Lateral and Longitudinal Spatial Correlation Coefficients and Frequency Spectra.*

The lateral spatial correlation coefficient is defined as,

$$R_{11}(o, r, o) = \frac{\overline{u(x, y)\, u(x, y+r)}}{(\overline{u^2(x, y)})^{\frac{1}{2}}\, (\overline{u^2(x, y+r)})^{\frac{1}{2}}} \tag{21}$$

and the longitudinal spatial correlation coefficient is defined as

$$R_{11}(r, o, o) = \frac{\overline{u(x, y)\, u(x+r, y)}}{(\overline{u^2(x, y)})^{\frac{1}{2}}\, (\overline{u^2(x+r, y)})^{\frac{1}{2}}}. \tag{22}$$

Figures 15 and 16 show $R_{11}(o, r, o)$ measurements at two longitudinal positions in the mixing layer with $U_2/U_1 = 0{\cdot}30$. As a further check upon the self-preservation of the mixing layer the measurements were made at the same values of $\bar{y}$ at each longitudinal position. The wire separation, $r$, is made dimensionless by the local length scale, $y'_{0{\cdot}1} - y'_{0{\cdot}9}$. It is seen that the distributions at each longitudinal position are similar which is a property of self-preservation. Small differences between the distributions occur when one wire is far from the mixing layer and these are explained by the interference of the boundary layer on the roof of the tunnel which was indicated by the $\overline{u^2}$ measurements for $x' > 0{\cdot}60$ m. The measurements for $x = 0{\cdot}34$ m are therefore assumed to be representative of the self-preserving mixing layer with $U_2/U_1 = 0{\cdot}30$. Figure 15 includes some of the measurements of Bradshaw et al[21] for the mixing layer region of a round free jet and the distributions are in agreement with present measurements for $\dfrac{r}{y'_{0{\cdot}1} - y'_{0{\cdot}9}} < 0{\cdot}5$.

Fig. 17 shows $R_{11}$ $(o, r, o)$ measurements in the self-preserving region of the mixing layer with $U_2/U_1 = 0{\cdot}61$. The measurements shown in Fig. 17 are for lateral positions in the mixing layer which have the same values of the dimensionless mean velocity $(U - U_2)/(U_1 - U_2)$ as those used for $U_2/U_1 = 0{\cdot}30$. A comparison of Figs. 15 and 17 indicates that differences exist between the turbulence structures of the two mixing layers. These differences are more easily seen by replotting $R_{11}$ $(o, r, o)$ measurements as contours in the $\left(\dfrac{r}{y'_{0{\cdot}1} - y'_{0{\cdot}9}}, \bar{y}\right)$ plane (Figs. 18 and 19). For small wire separation distances $\left(\dfrac{r}{y'_{0{\cdot}1} - y'_{0{\cdot}9}} < 0{\cdot}5 \text{ say}\right)$ the contours for both of the mixing layers are approximately parallel to the $\bar{y}$ axis across most of the widths of the mixing layers. This indicates that the medium scale, energy containing turbulence may be approximately homogeneous across the mixing layers.

It is seen that contours for $U_2/U_1 = 0{\cdot}61$ are more widely spaced than the equivalent contours for $U_2/U_1 = 0{\cdot}30$ which suggests that $y'_{0{\cdot}1} - y'_{0{\cdot}9}$ is not a suitable length for scaling the medium scale turbulence. The use of the length scale, $b = Ax/\sigma$ (from Ref. 16) greatly reduces this discrepancy and this is a further justification of the new constant eddy viscosity hypothesis (Yule[16]).

Figs. 18 and 19 indicate that the large eddy motions of the two mixing layers differ markedly. This is evident from the negative correlation trough which extends to much higher values of $\bar{y}$ for $U_2/U_1 = 0{\cdot}61$ than for $U_2/U_1 = 0{\cdot}30$ and is indicative of a relatively stronger periodic large eddy motion at the higher velocity ratio.

Fig. 20 shows $R_{11}$ $(r, o, o)$ measurements at three transverse positions in the self-preserving region of the mixing layer with $U_2/U_1 = 0{\cdot}61$. The measurements of Bradshaw et al at the same values of $\bar{y}$ in the mixing layer of a round free jet are included in the figure. The distributions for $U_2/U_1 = 0{\cdot}61$ are seen to coincide for $\dfrac{r}{y'_{0{\cdot}1} - y'_{0{\cdot}9}} < 0{\cdot}5$ approximately which again infers a homogeneous lateral distribution of the medium scale turbulence. If the $R_{11}$ $(r, o, o)$ measurements for $U_2/U_1 = 0{\cdot}61$ are compared with the associated $R_{11}$ $(o, r, o)$ measurements (Fig. 17) it is seen that any value of $R_{11}$ $(r, o, o)$ occurs at approximately twice the magnitude of $\dfrac{r}{y'_{0{\cdot}1} - y'_{0{\cdot}9}}$ at which the same value of $R_{11}$ $(o, r, o)$ occurs (for $\dfrac{r}{y'_{0{\cdot}1} - y'_{0{\cdot}9}} < 0{\cdot}5$). This proportionality is a property of isotropic turbulence and it infers that approximate local isotropy for the medium and small scale turbulence is possible.

The present measurements and Bradshaw's measurements agree at the centre of the mixing layer (at $\bar{y} = 0{\cdot}27$) but do not agree at the edges of the layer. The differences are most likely due to the axisymmetric nature of Bradshaw's flow. This axisymmetry is expected to be most strongly reflected in the longitudinal correlations and it may result in a stretching of the eddies at the outside of the jet and an opposite effect upon the eddies at the inner edge of the mixing layer. Bradshaw's curves for the inner and outer edges of the mixing layers are in qualitative agreement with this.

Frequency spectra of the $\overline{u^2}$ intensity component were measured in the mixing layer with $U_2/U_1 = 0{\cdot}61$ at $x' = 0{\cdot}57$ m and at transverse positions which had the same values of $(U - U_2)/(U_1 - U_2)$ as the positions at which Bradshaw measured spectra in the mixing layer of a round free jet. The same non-dimensional frequency as that of Bradshaw is used to present the measurements, i.e. $\omega x/U_1$ where $\omega$ is the angular frequency. Following Bradshaw the spectral density of $\overline{u^2}$, $F_{11}$, is normalised so that

$$\int_0^\infty F_{11}\, d\left(\frac{\omega x}{U_1}\right) = 1. \tag{23}$$

The present measurements and those of Bradshaw are shown in Fig. 21.

It is seen that the spectra for the mixing layer with $U_2/U_1 = 0{\cdot}61$ are at higher values of the non-dimensional frequency than those for $U_2/U_1 = 0$. This is expected because of the higher convection velocities at the higher velocity ratio. By converting the measured frequency spectra into the approximate one-dimensional wave number spectra the effect of the differing convection velocities is removed and an approximation of the distribution of the turbulent energy in the different eddy sizes is obtained. Thus the structures of the turbulence in the two mixing layers may be compared directly.

If it is assumed that all the turbulent eddies at a point in a mixing layer are convected along with the same mean convection velocity, $\overline{U}_c$, then the one-dimensional wave number component $k_x$ and the frequency are related by

$$k_x = \frac{\omega}{\overline{U}_c}. \tag{24}$$

In fact turbulent eddies of a certain size can possess a wide range of convection velocities but Wills[22] measured the convection velocities in the mixing layer of a round free jet and his measurements indicate that the assumption of a mean convection velocity which is independent of eddy size is a reasonable approximation. Both Wills and Bradshaw[23] et al reported identical distributions of $\overline{U}_c$ across the mixing layer of a round free jet. The method of finding the peak spatial covariance of the signals of two hot wires with a fixed time delay was used. Wills pointed out that $\overline{U}_c$ may be defined and measured in at least three different ways. However the full energy spectra of Wills and of Bradshaw (which were measured at two different positions in the same mixing layer) show that the different definitions yield essentially the same values for $\overline{U}_c$. It was found that $\overline{U}_c$ varied from being 20 per cent less than $U$ at the inner edge of the mixing layer to being 20 per cent of $U_1$ greater than $U$ at the outer edge.

The normalised one-dimensional wave number spectra, $\phi_{11}$ for the free mixing layer have been derived from Bradshaw's frequency spectra by using the $U_c$ distribution given by Wills and Bradshaw and equation (24). The spectra are normalised to aid comparison between measurements at different transverse positions and also for comparison with the measurements for $U_2/U_1 = 0{\cdot}61$ so that

$$(y'_{0{\cdot}1} - y'_{0{\cdot}9}) \int_0^\infty \phi_{11}\, dk_x = 0 \tag{25}$$

Measurements of $\overline{U}_c$ have not been made in the present experiments but since the variation in mean

velocity across the mixing layer is small compared with the absolute mean velocities it is reasonable to assume that the differences between the local values of $\overline{U}_c$ and $U$ are also small compared with the differences found in the free mixing layer. Thus the wave number spectra for $U_2/U_1 = 0{\cdot}61$ (Fig. 2) have been derived from the frequency spectra by assuming that $\overline{U}_c = U$ in equation (24).

Considering each mixing layer separately it is seen that wave number spectra for different lateral positions in a mixing layer collapse on each other outside the low wave number range. This supports the suggestion of approximate homogeneity for the lateral distribution of the medium and small scale turbulence which was inferred from the spatial correlation coefficient measurements.

The Universal Equilibrium Theory of Kolmogoroff proposes that at high Reynolds numbers an inertial subrange might exist in the spectra between the energy containing and energy dissipating wave numbers and in this subrange dimensional arguments show that for isotropic turbulence

$$\phi_{11} = \text{constant} \times k_x^{-5/3}. \tag{26}$$

This proportionality is included in Fig. 22 and the experimental spectra are seen to approach the power law relation closely. This must not be taken as proof that the assumptions involved in the Universal Equilibrium Theory are valid for the two mixing layer flows (see for example Gibson[24]). However the spectra and spatial correlation measurements described above are all consistent with approximately locally isotropic and laterally homogeneous distributions of the medium scale turbulence and the small scale energy dissipating turbulence.

The wave number spectra of the mixing layers with velocity ratios, $U_2/U_1 = 0$ and $U_2/U_1 = 0{\cdot}61$, are now compared. Fig. 22 indicates that at similar mixing layer widths comparatively more of the turbulent energy is contained in the larger eddies at the higher velocity ratio. Thus the larger eddies appear to increase in strength relative to the rest of the turbulent motion as the velocity ratio, $U_2/U_1$, increases. It will be recalled that the $R_{11}(o, r, o)$ measurements in the mixing layers with $U_2/U_1 = 0{\cdot}30$ and $U_2/U_1 = 0{\cdot}61$ also indicated a stronger large eddy motion at the higher velocity ratio. Furthermore the peaks in the wave number spectra are indicative of a strong, periodic large eddy motion which is not so pronounced at the lower velocity ratio. Wave number spectra[18] were also derived by integration of the $R_{11}(r, o, o)$ curves using a curve fitting technique. These curves are not included in Fig. 22 for reasons of clarity but there was good agreement with the curves derived from the measured frequency spectra. A discussion of the turbulent energy balances obtained from the present measurements will be given in a subsequent paper.

8. *Conclusions.*

The magnitudes of the non-dimensional turbulence components in a mixing layer, $(\overline{u^2})^{\frac{1}{2}}/(U_1 - U_2)$, $(\overline{v^2})^{\frac{1}{2}}/(U_1 - U_2)$ and $(\overline{w^2})^{\frac{1}{2}}/(U_1 - U_2)$ are observed to increase with increasing velocity ratio, $U_2/U_1$. The peak non-dimensional total turbulence intensity increases by 80 per cent from $U_2/U_1 = 0$ to $U_2/U_1 = 0{\cdot}61$.

The presence of a secondary stream has most effect upon the large eddy motion in a mixing layer and an increase in the large eddy strength relative to the rest of the turbulence is indicated for increasing $U_2/U_1$.

The medium and small scale turbulence has approximately homogeneous and locally isotropic lateral distributions across a mixing layer.

## LIST OF SYMBOLS

| | |
|---|---|
| $A$ | Constant in equation (16) |
| $b$ | Local length scale of mixing layer |
| $f$ | Self-preserving mean velocity in eddy viscosity analysis |
| $f$ | Self-preserving mean velocity in terms of the variable $\eta$ |
| $F_{11}$ | Normalised frequency spectra of $u^2$ equation (23) |
| $\bar{g}$ | Self-preserving form of shear-stress in terms of the variable $\eta$ |
| $k_x$ | $x$-direction wave number component |
| $K_G$ | Coefficient in equation (10) |
| $K_Y$ | Coefficient in equation (18) |
| $\overline{q}^2$ | $\overline{q}^2 = \overline{u}^2 + \overline{v}^2 + \overline{w}^2$ |
| $r$ | Distance between hot wires |
| $R_{11}(o, r, o)$ | Lateral spatial correlation coefficient |
| $R_{11}(r, o, o)$ | Longitudinal spatial correlation coefficient |
| $\overline{u}^2$ | $x$ component of turbulence intensity |
| $U$ | $x$ component of mean velocity |
| $\overline{U}_c$ | Mean convection velocity |
| $\overline{v}^2$ | $y$ component of turbulence intensity |
| $V$ | $y$ component of mean velocity |
| $\overline{w^2}$ | $z$ component of turbulence intensity |
| $(x, y, z)$ | Coordinate system for self-preserving mixing |
| $(x', y', z')$ | Experimental coordinate system |
| $\bar{y}$ | $\bar{y} = \dfrac{y' - y'_{0\cdot9}}{y'_{0\cdot1} - y'_{0\cdot9}}$ |
| $\delta$ | Mixing layer width |

| | |
|---|---|
| $\delta^* \delta^{**}$ | Displacement and momentum thickness |
| $\zeta$ | $\zeta = \sigma y/x$ |
| $\eta$ | $\eta = y/x$ |
| $\nu_T$ | Eddy viscosity |
| $\sigma$ | Similarity parameter, *see* equations (13) and (18) |
| $\phi_{11}$ | Normalised one-dimensional wave number spectra |
| $\psi$ | Stream function |
| $\omega$ | Frequency (radians/s) |

*Subscripts*

| | |
|---|---|
| 0·1 | Refers to values at $f = 0{\cdot}1$ |
| 0·9 | Refers to values at $f = 0{\cdot}9$ |
| 1 | Refers to values in the primary stream |
| 2 | Refers to values in the secondary stream |

N.B. double subscripts denote tensor components.

---

## REFERENCES


| *No.* | *Author(s)* | *Title, etc.* |
|---|---|---|
| 1 | J. O. Hinze . . . . . | *Turbulence* McGraw-Hill, New York (1950). |
| 2 | W. Tollmien . . . . . | Calculation of turbulent expansion processes. *ZAAM* Vol. 6, page 468 (1926). |
| 3 | A. M. Kuethe . . . . . | Investigation of turbulent mixing regions formed by jets. *ASME Trans* Vol. 57, page A87 (1935). |
| 4 | H. Görtler . . . . . | Berechnung von aufgaben der frein turbulenz auf grund eines neuen nahrungsansatzes. *ZAAM* Vol. 22, No. 5 pp. 244–254 (1942). |
| 5 | H. W. Liepmann and J. Laufer . . | Investigations of free turbulent mixing. NACA TN 1257 (1947). |
| 6 | M. L. Albertson, Y. B. Dai R. A. Jensen and H. Roose . . | Diffusion of submerged jets. *Proc. Am. Soc. Civil Engrs.* Vol. 74, page 1751 (1948). |

| No. | Author(s) | Title, etc. |
|---|---|---|
| 7 | L. Ting .. .. .. | On the mixing of two parallel streams. *Journal of Mathematics and Physics* 38 page 153 (1959). |
| 8 | R. D. Mills .. .. .. | Numerical and experimental investigations of the shear layer between two parallel streams. *J.F.M.* Vol. 33, pp. 591–616 (1968). |
| 9 | R. L. Baker and H. Weinstein | Analytical investigation of the mixing of two parallel streams of dissimilar fluids. NASA CR-956 (1968). |
| 10 | R. L. Baker and H. Weinstein | Experimental investigation of the mixing of two parallel streams of dissimilar fluids. NASA CR-957 (1968). |
| 11 | O. V. Yakovlevskiy .. .. | The problem of the thickness of the turbulent mixing zone on the boundary between two gas streams of different velocity and density. Isv. Akad. Nauk. SSSR Otd Tekh Nauk (1958). |
| 12 | G. N. Abramovich .. .. | *The theory of turbulent jets.* M.I.T. press (1963). |
| 13 | C. M. Sabin .. .. .. | An analytical and experimental study of the plane incompressible turbulent shear layer with arbitrary velocity ratio and pressure gradient. *ASME Trans Journal of Basic Engineering* Vol 86, series D page 421 (1965). |
| 14 | J. B. Miles and J. S. Shih .. | Similarity parameter for two stream turbulent jet mixing region. *AIAA Journal* Vol. 6, pp 1429–1430 (1968). |
| 15 | I. Wygnanski and H. E. Fiedler .. .. | The two-dimensional mixing region. *JFM* Vol. 41, pp. 327–361 (1970). |
| 16 | A. J. Yule .. .. .. | The spreading of turbulent mixing layers. (to be published). |
| 17 | A. A. Townsend .. .. | *The structure of turbulent shear flow.* Cambridge University Press (1956). |
| 18 | A. J. Yule .. .. .. | Experimental and analytical investigations of two types of turbulent mixing flow. Ph.D. Thesis University of Manchester (1969). |
| 19 | P. O. A. L. Davies and H. H. Bruün .. | The performance of a yawed hot wire. Proc. Symp. on Instrumentation and Data Processing for Industrial Aerodynamics Paper 10, NPL (1968). |

20 L. J. S. Bradbury . . . . The structure of a self-preserving turbulent plane jet. *JFM* Vol. 23, pp. 31–61 (1965).

21 P. Bradshaw, D. H. Ferriss and R. F. Johnson . . . . Turbulence in the noise producing region of a circular jet. *JFM* Vol. 19, pp. 591–624 (1964).

22 J. A. B. Wills . . . . On convection velocities in turbulent shear flows. *JFM* Vol. 20, pp. 417–432 (1964).

23 P. Bradshaw and D. H. Ferriss . . . . The spectral energy balance in a turbulent mixing layer. ARC CP 899 (1965).

24 M. M. Gibson . . . . Spectra of turbulence in a round jet. *JFM* Vol. 15, pp. 161–173 (1963).

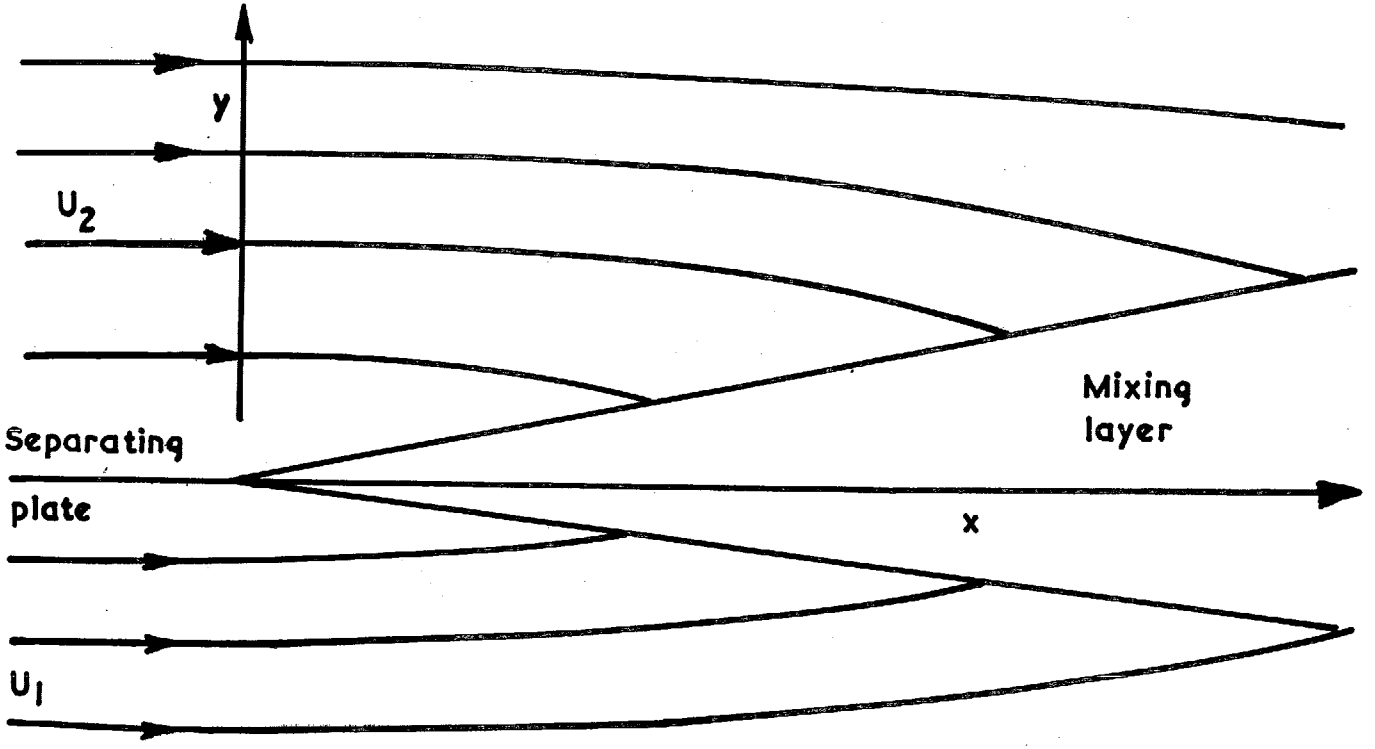


FIG. 1. The mixing of semi-infinite parallel streams.

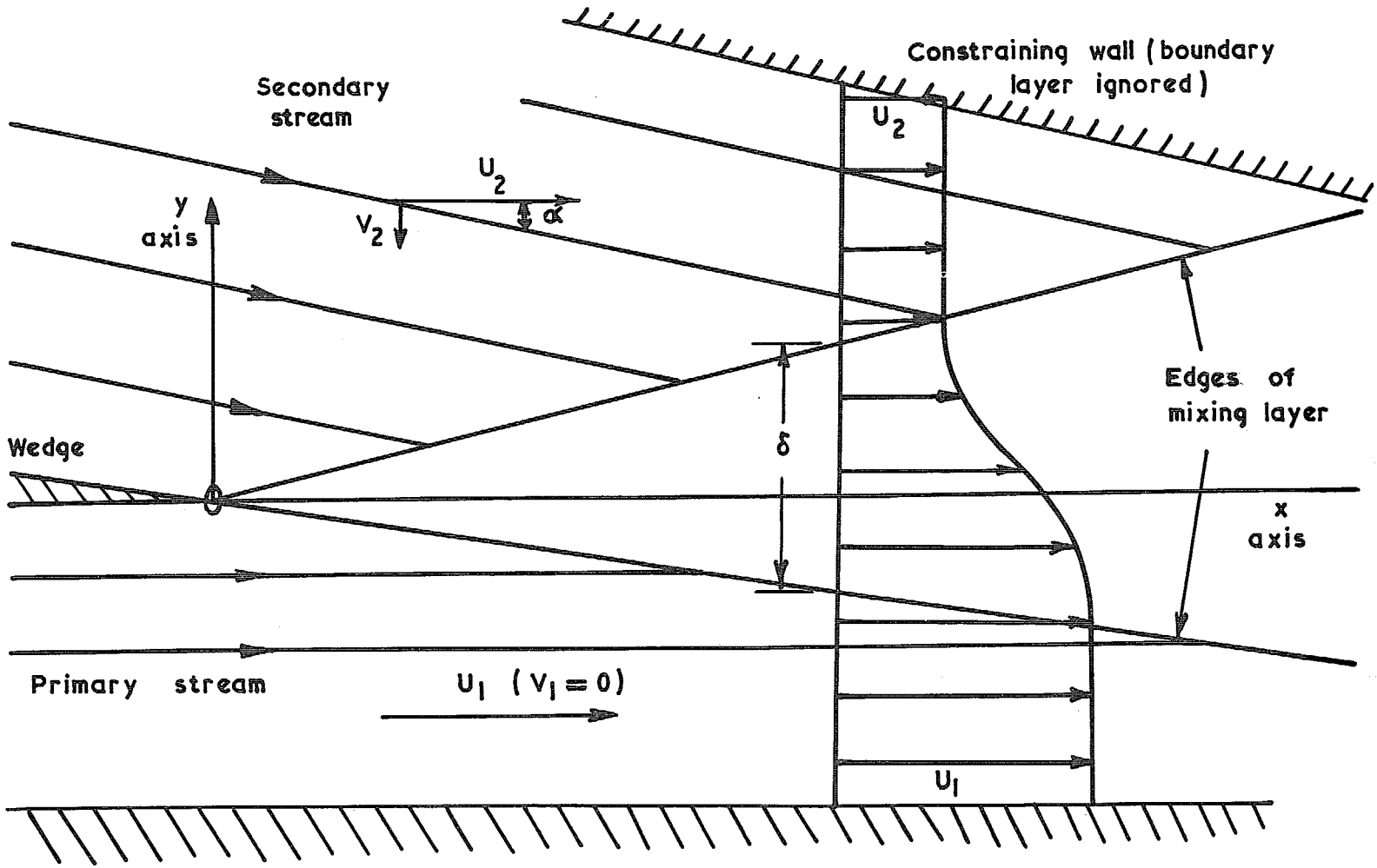


FIG. 2. Ideal self-preserving mixing.

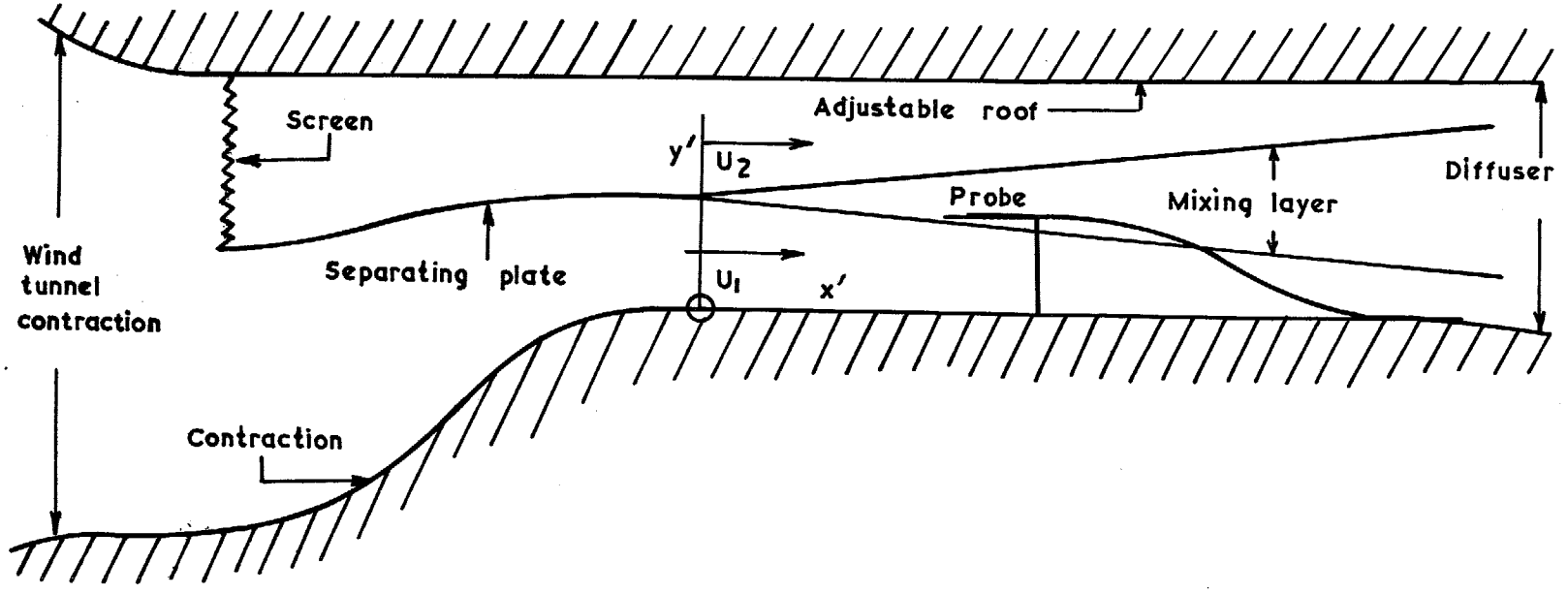


FIG. 3. Installation in working section of wind tunnel.

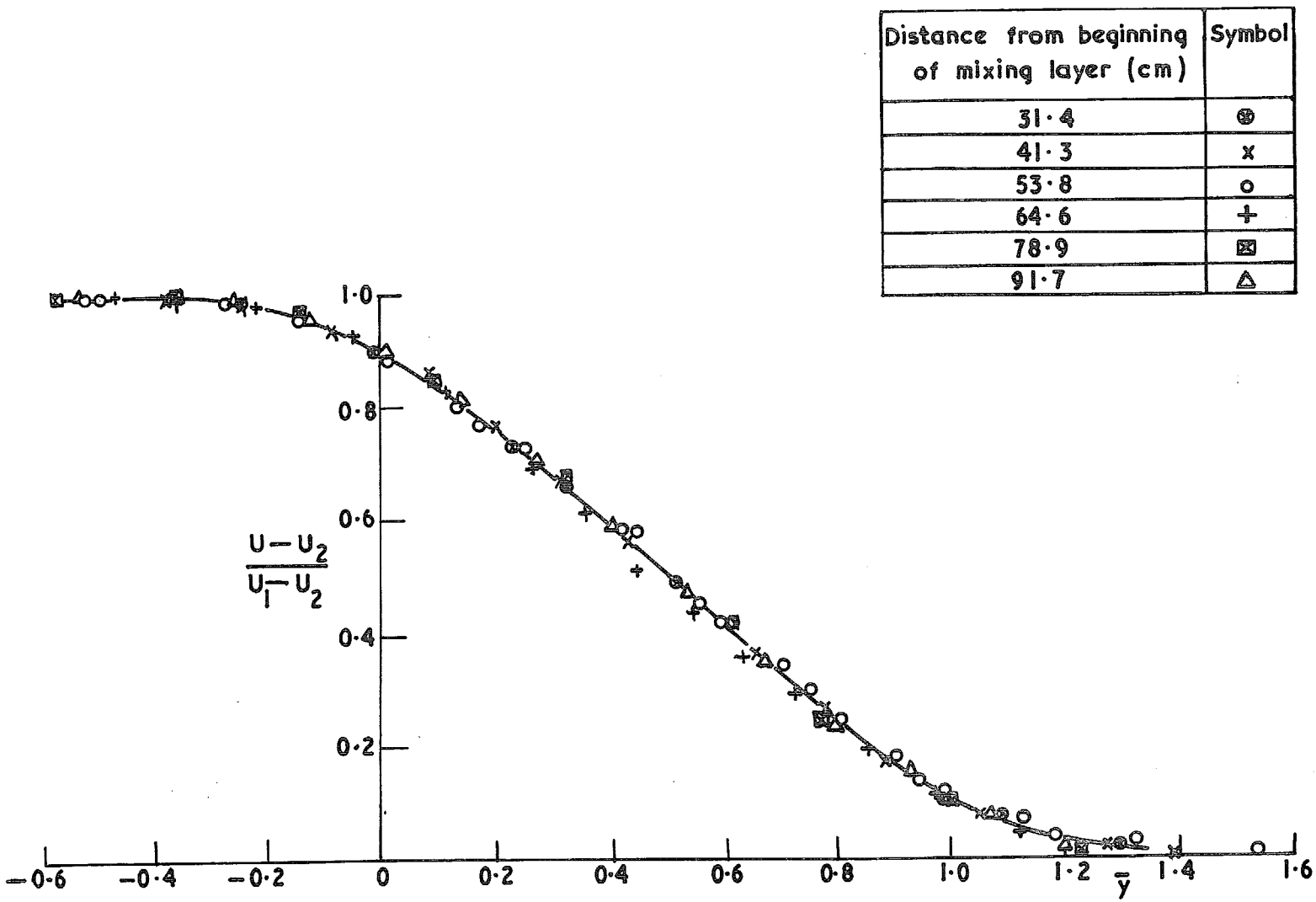


FIG. 4. Mean velocity measurements; $U_2/U_1 = 0{\cdot}61$.

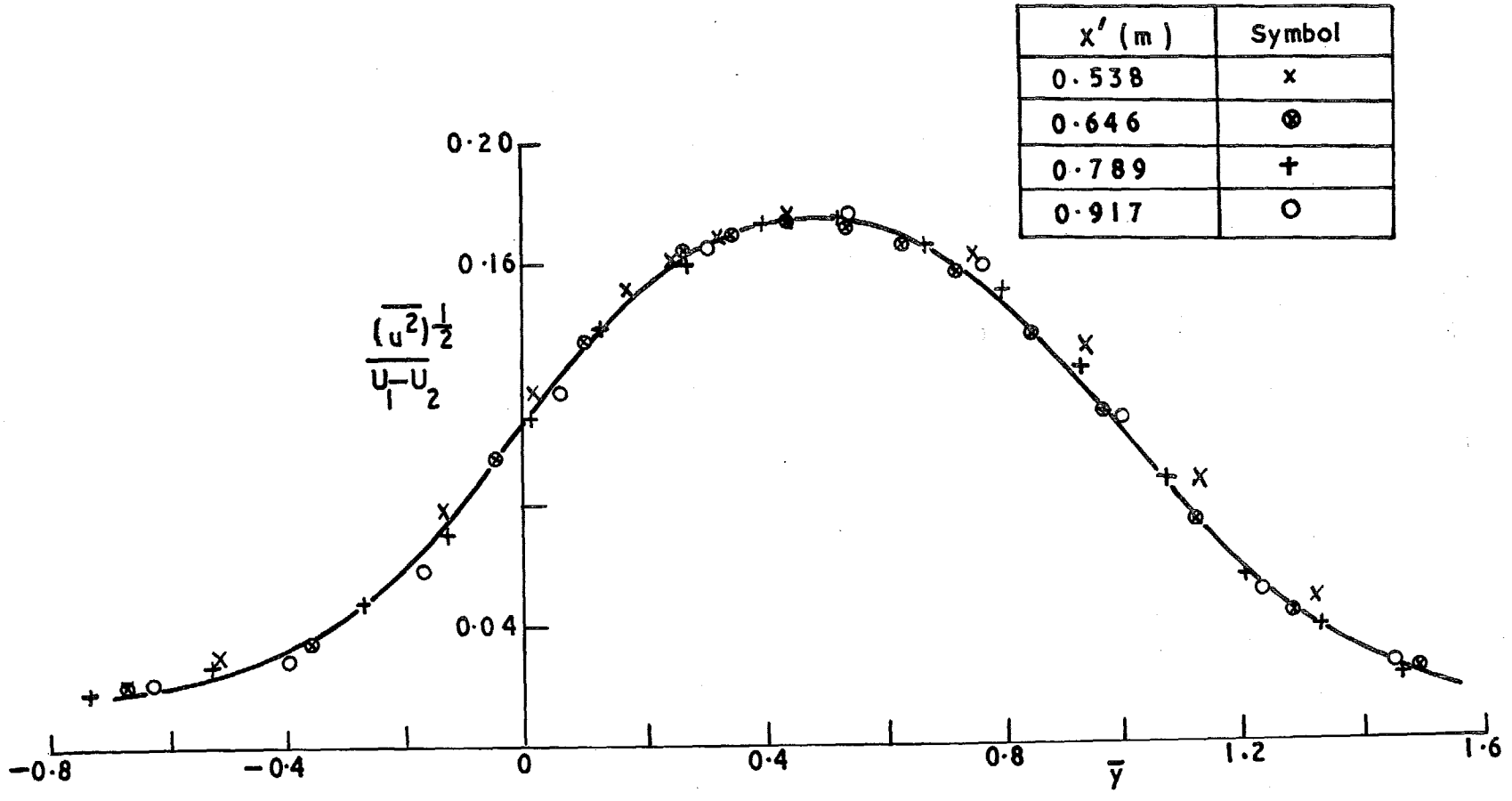


FIG. 5. Distributions of $(\overline{u^2})^{\frac{1}{2}}/(U_1-U_2)$.

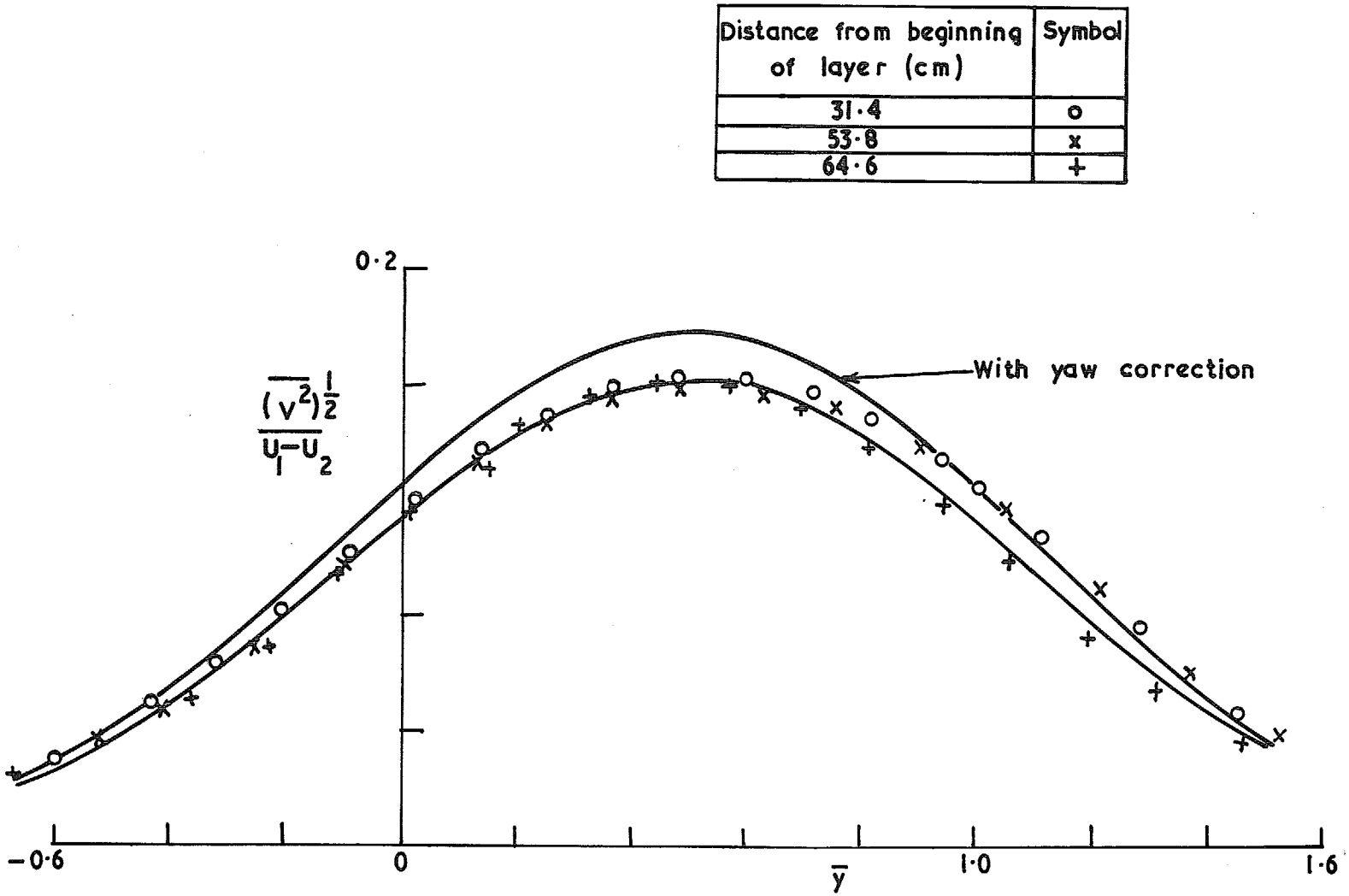


FIG. 6. Distribution of $(\overline{v^2})^{\frac{1}{2}}/(U_1-U_2)$, $U_2/U_1 = 0{\cdot}61$.

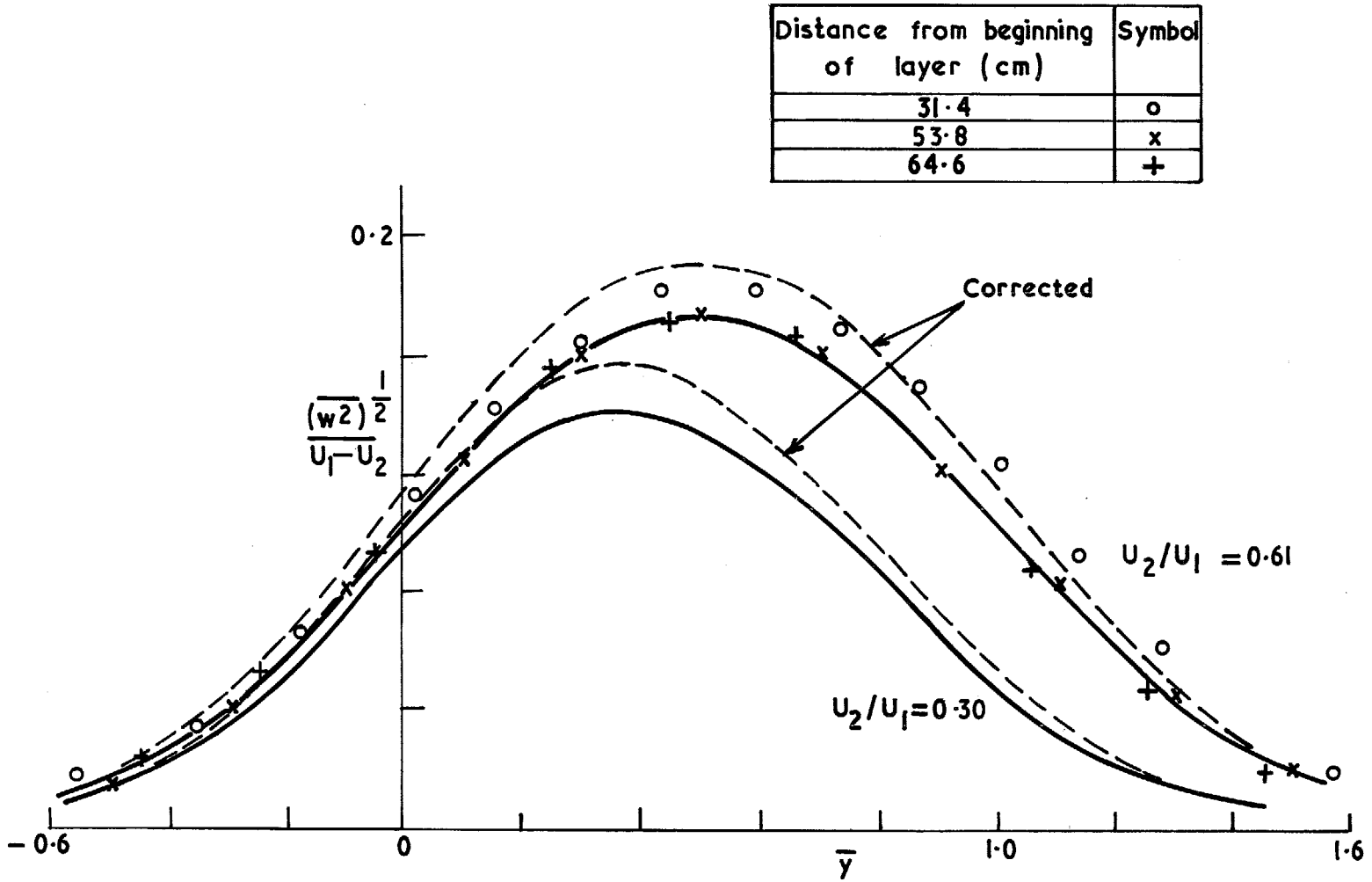


FIG. 7. Distributions of $(\overline{w^2})^{\frac{1}{2}}/(U_1-U_2)$.

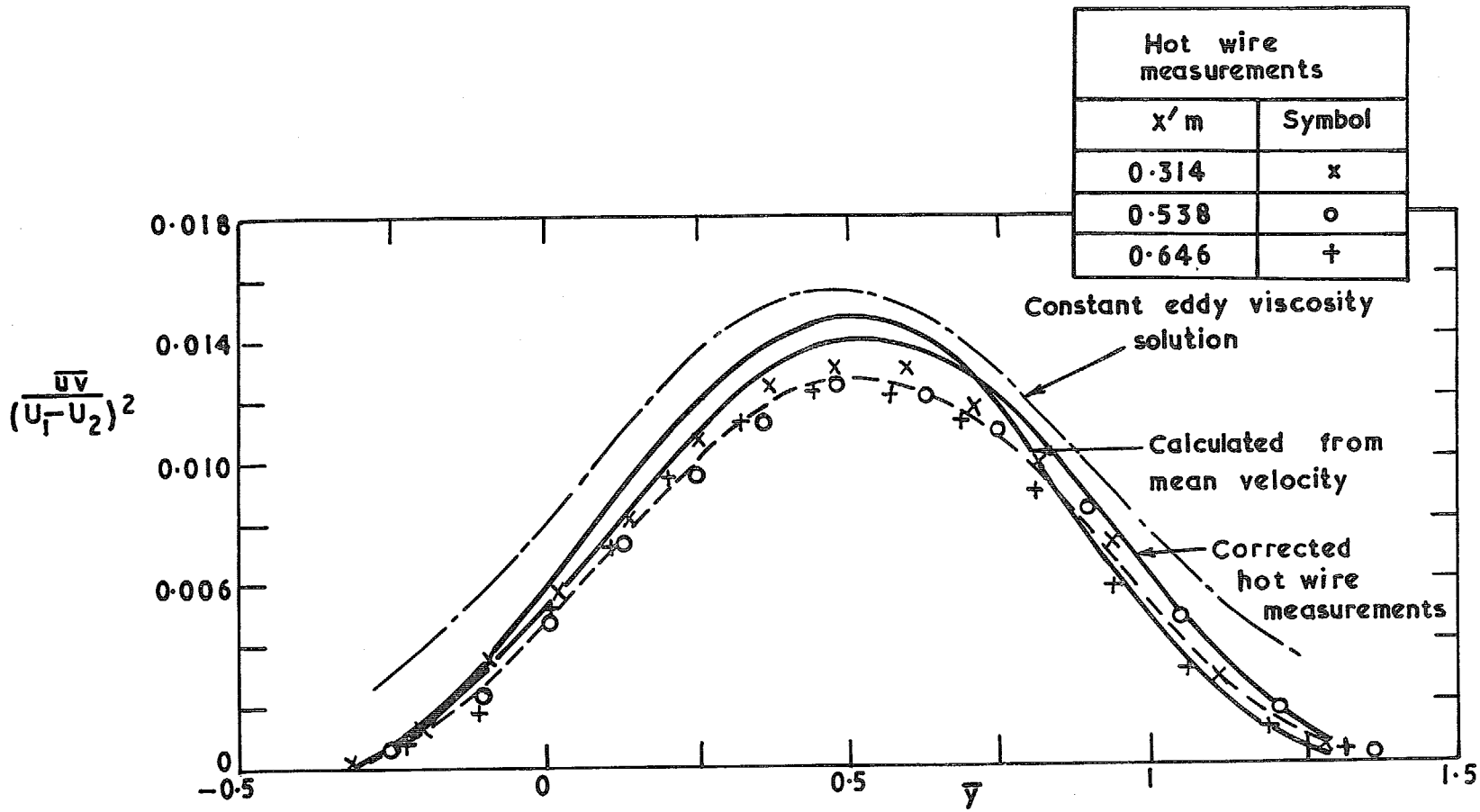


FIG. 8. The turbulent shear stress, $U_2/U_1 = 0{\cdot}61$.

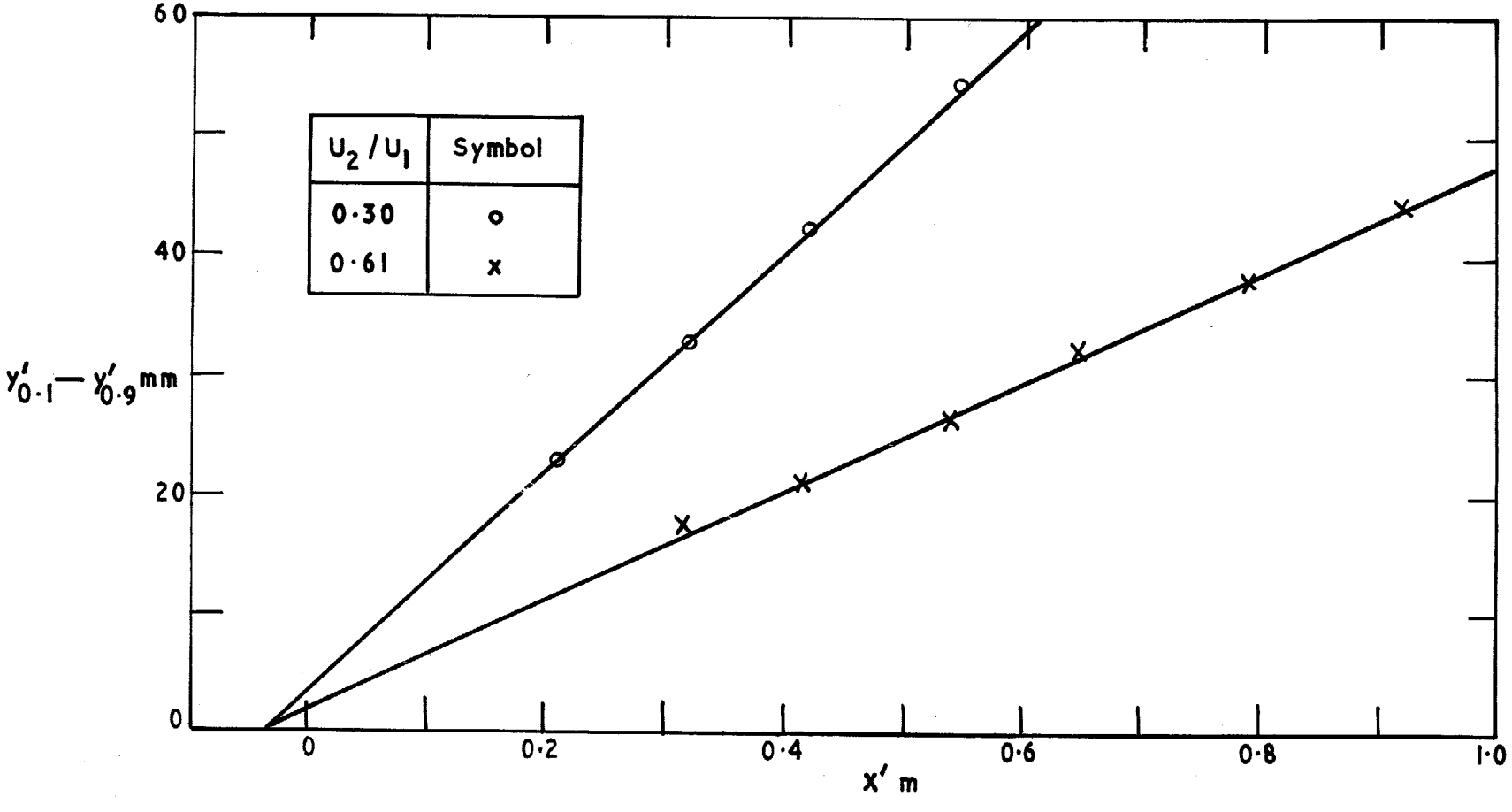


FIG. 9. Spreading rates of mixing layers.

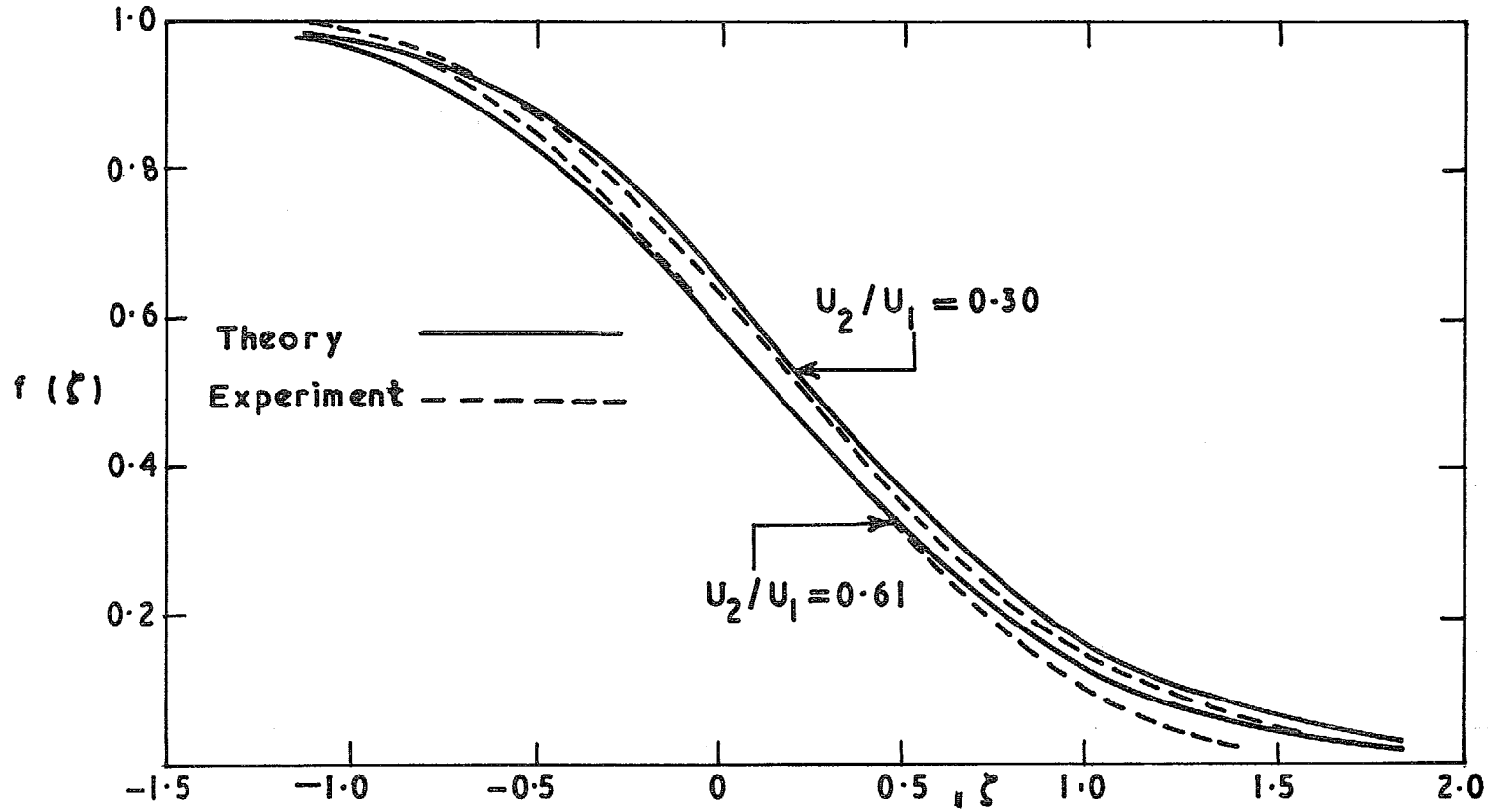


FIG. 10. Experimental and analytical velocity profiles.

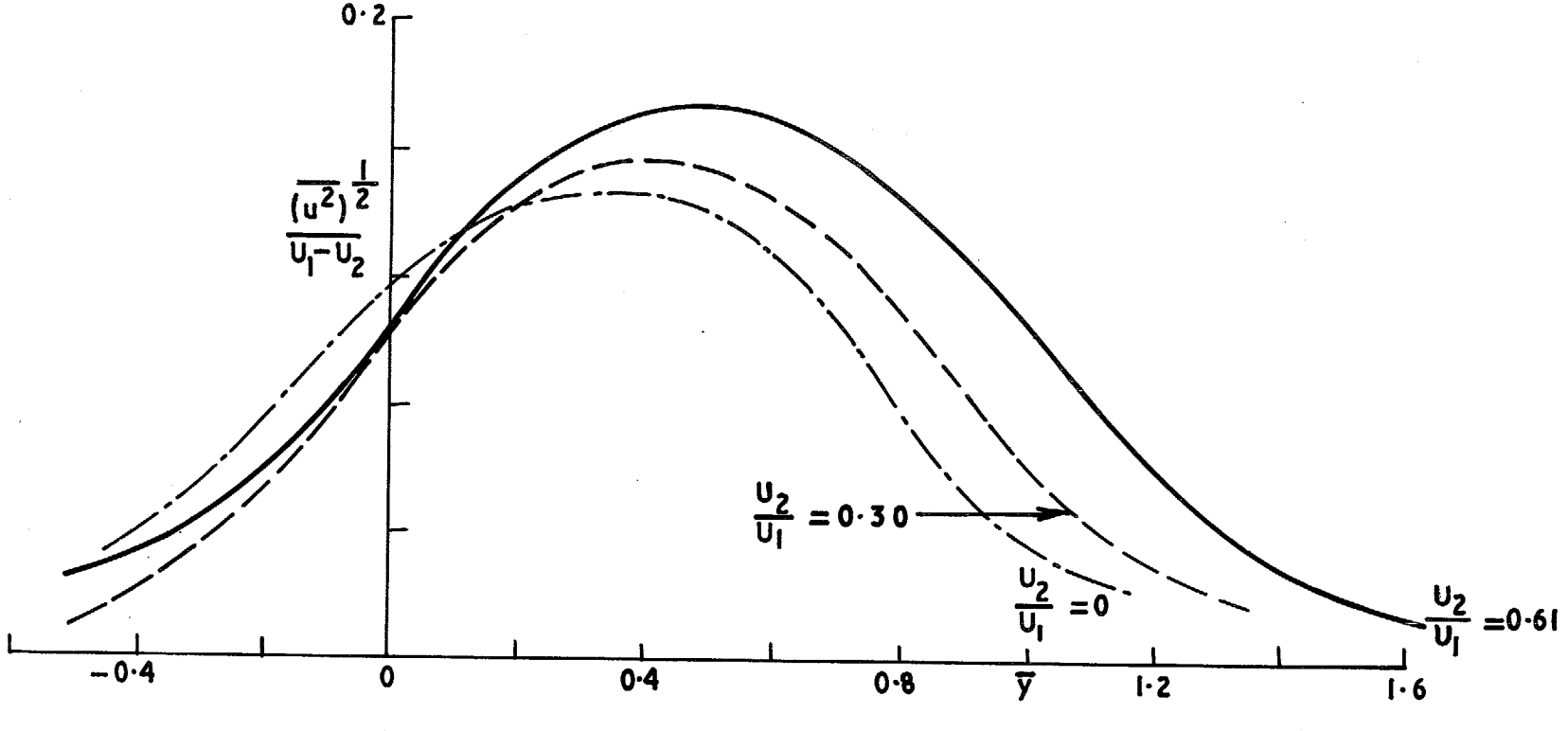


FIG. 11. Distributions of $(\overline{u^2})^{\frac{1}{2}}/(U_1-U_2)$.

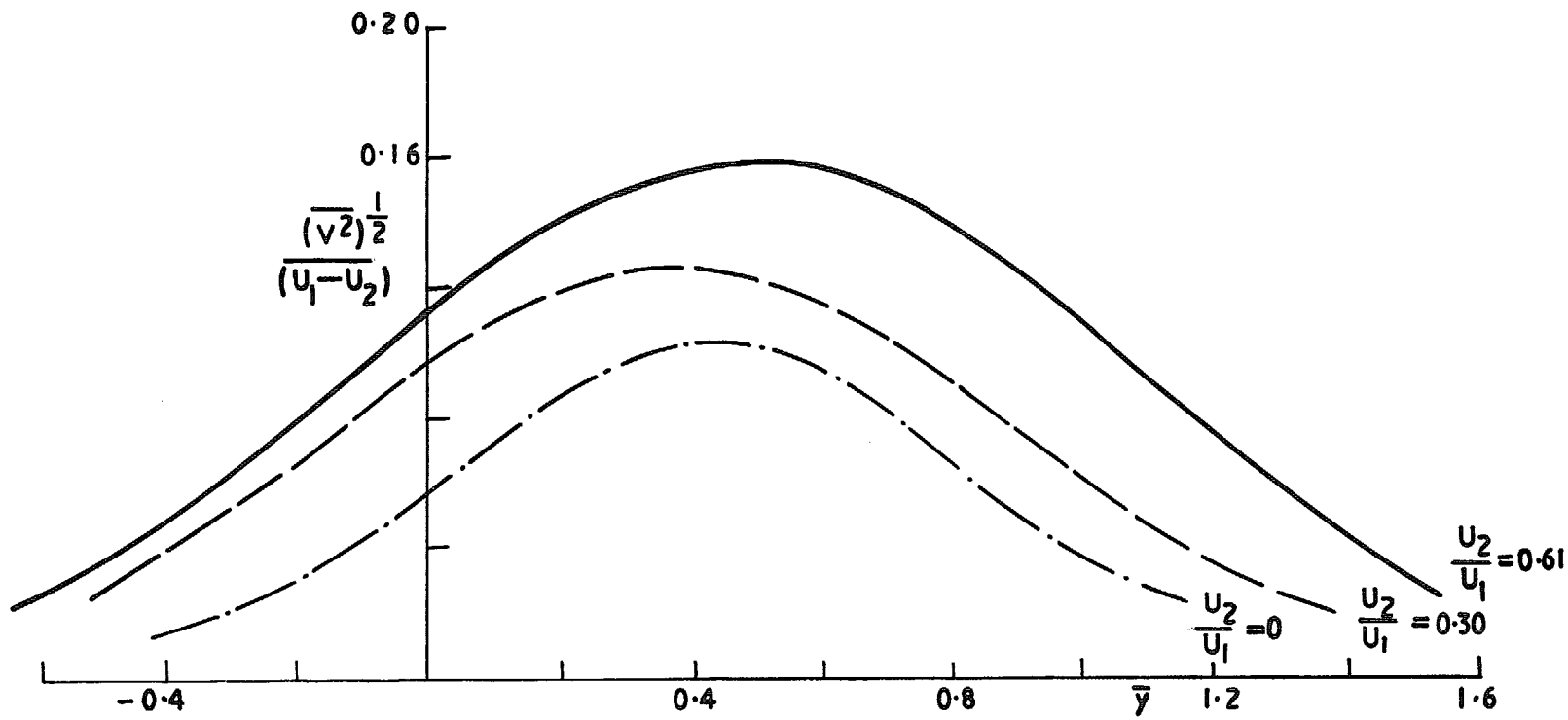


FIG. 12. Distributions of $(\overline{v^2})^{\frac{1}{2}}/(U_1-U_2)$.

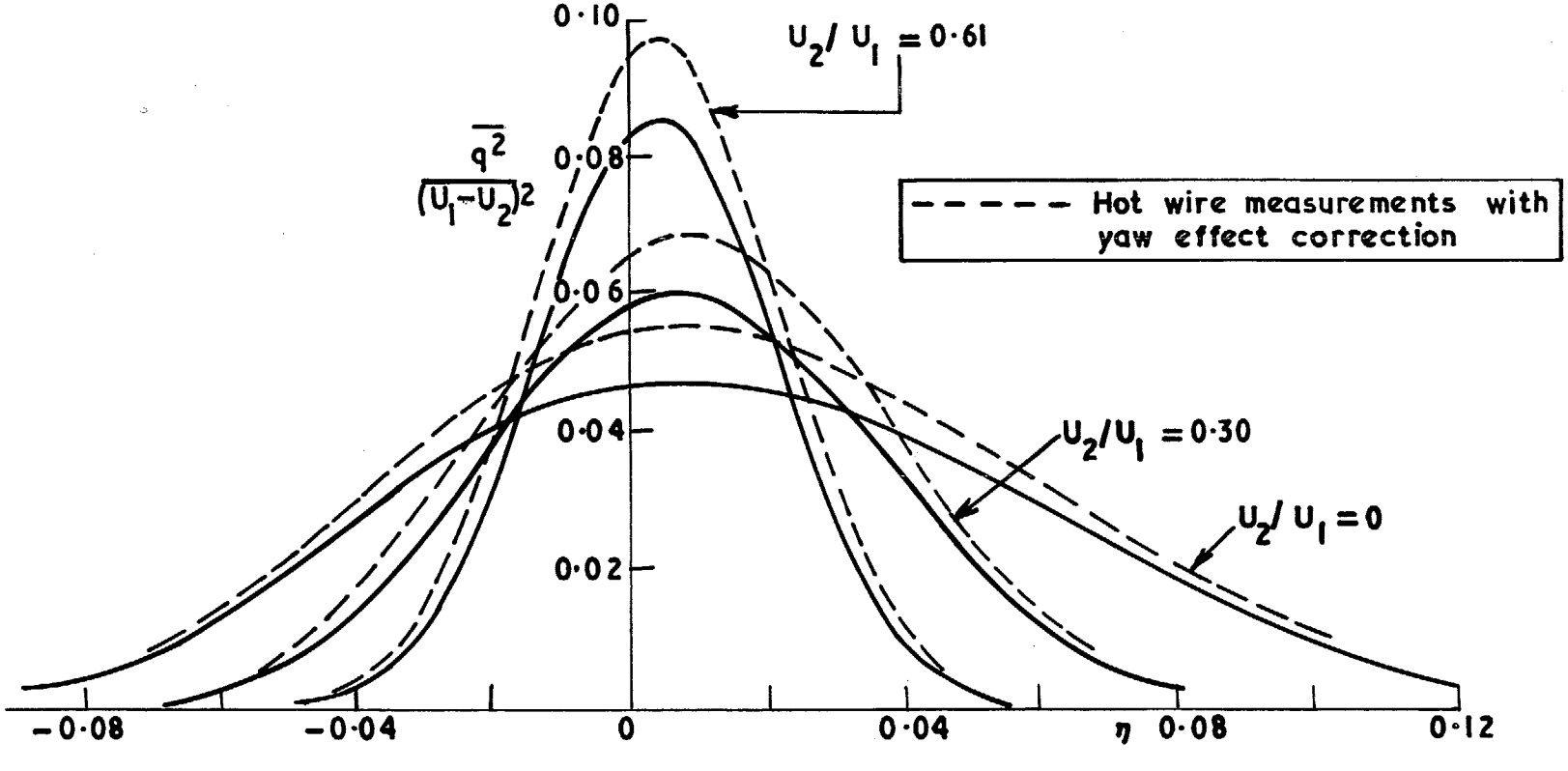


FIG. 13. Total turbulence intensity.

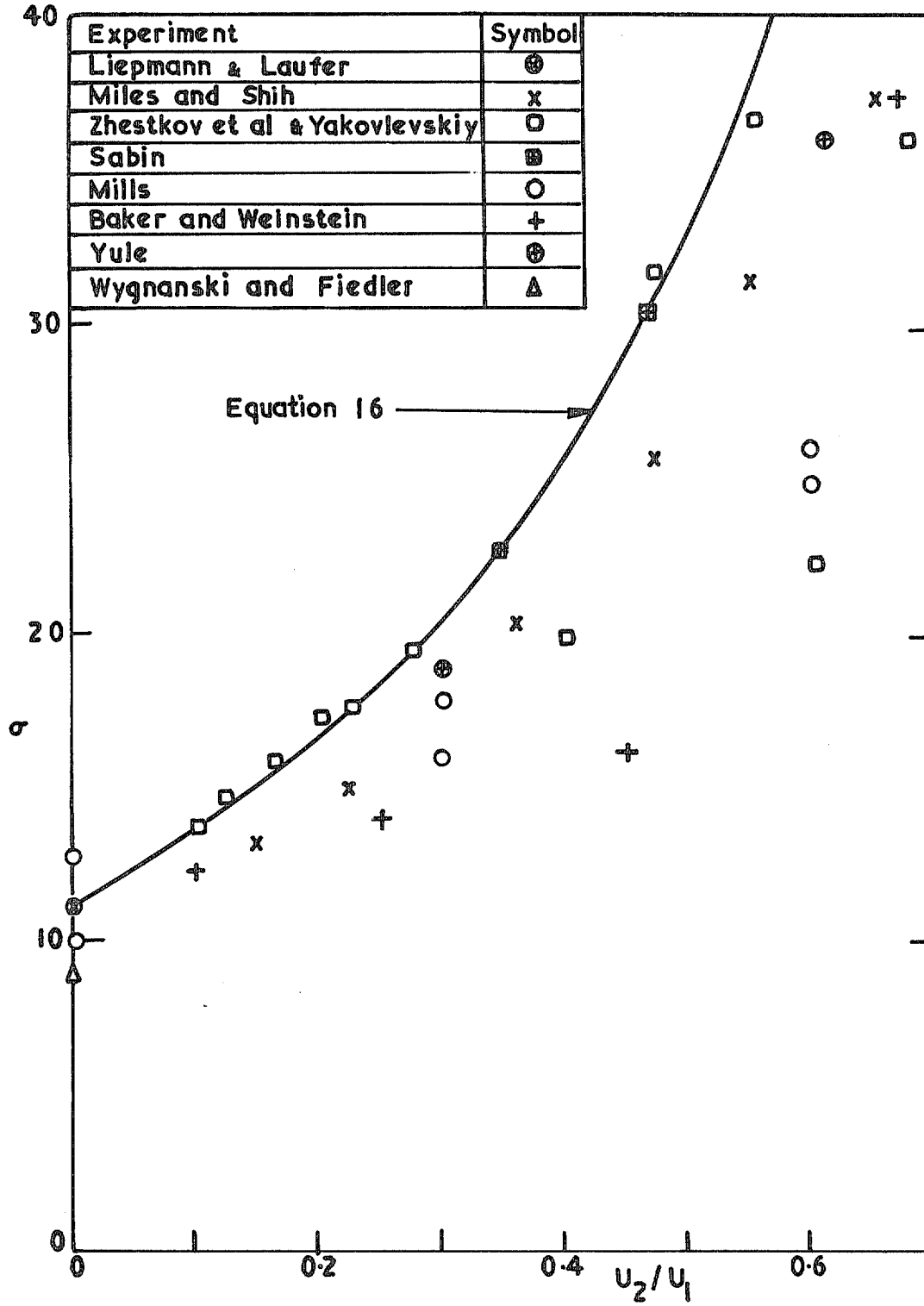


FIG. 14. Measurements of the similarity parameter.

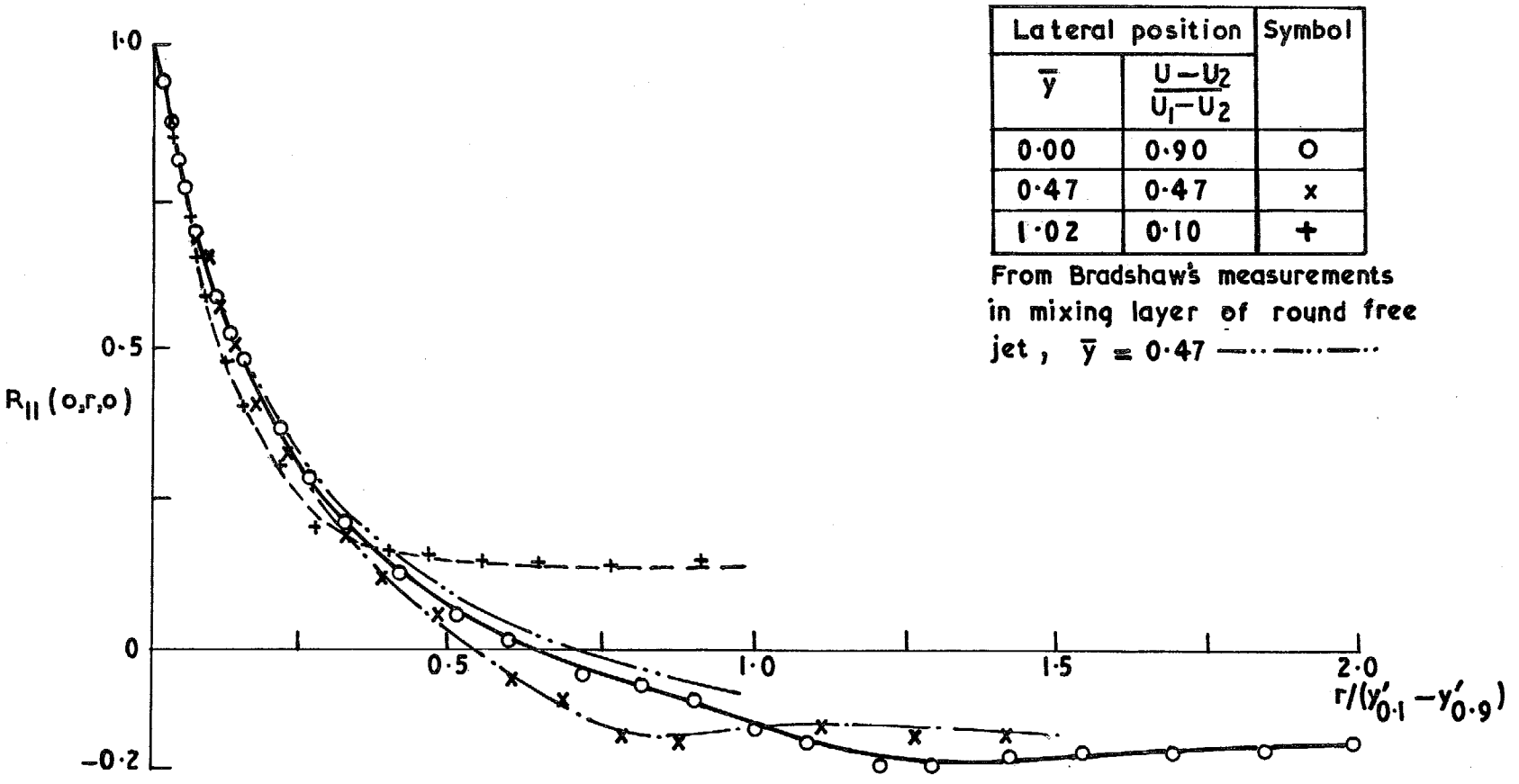


FIG. 15. Lateral correlation coefficient, $U_2/U_1 = 0{\cdot}30$, $x = 0{\cdot}34$ m.

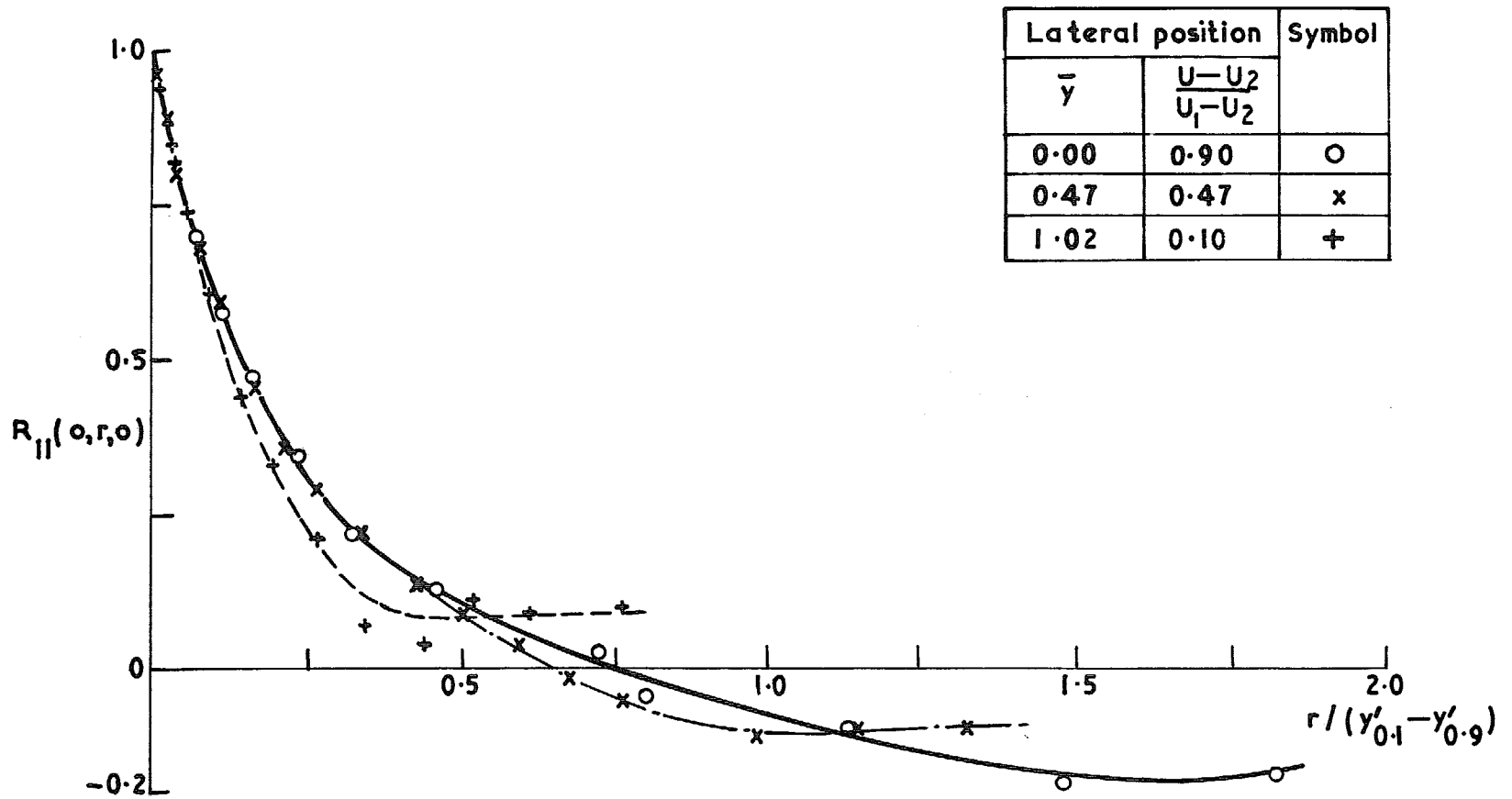


FIG. 16. Lateral correlation coefficient, $U_2/U_1 = 0{\cdot}30$, $x = 0{\cdot}68$ m.

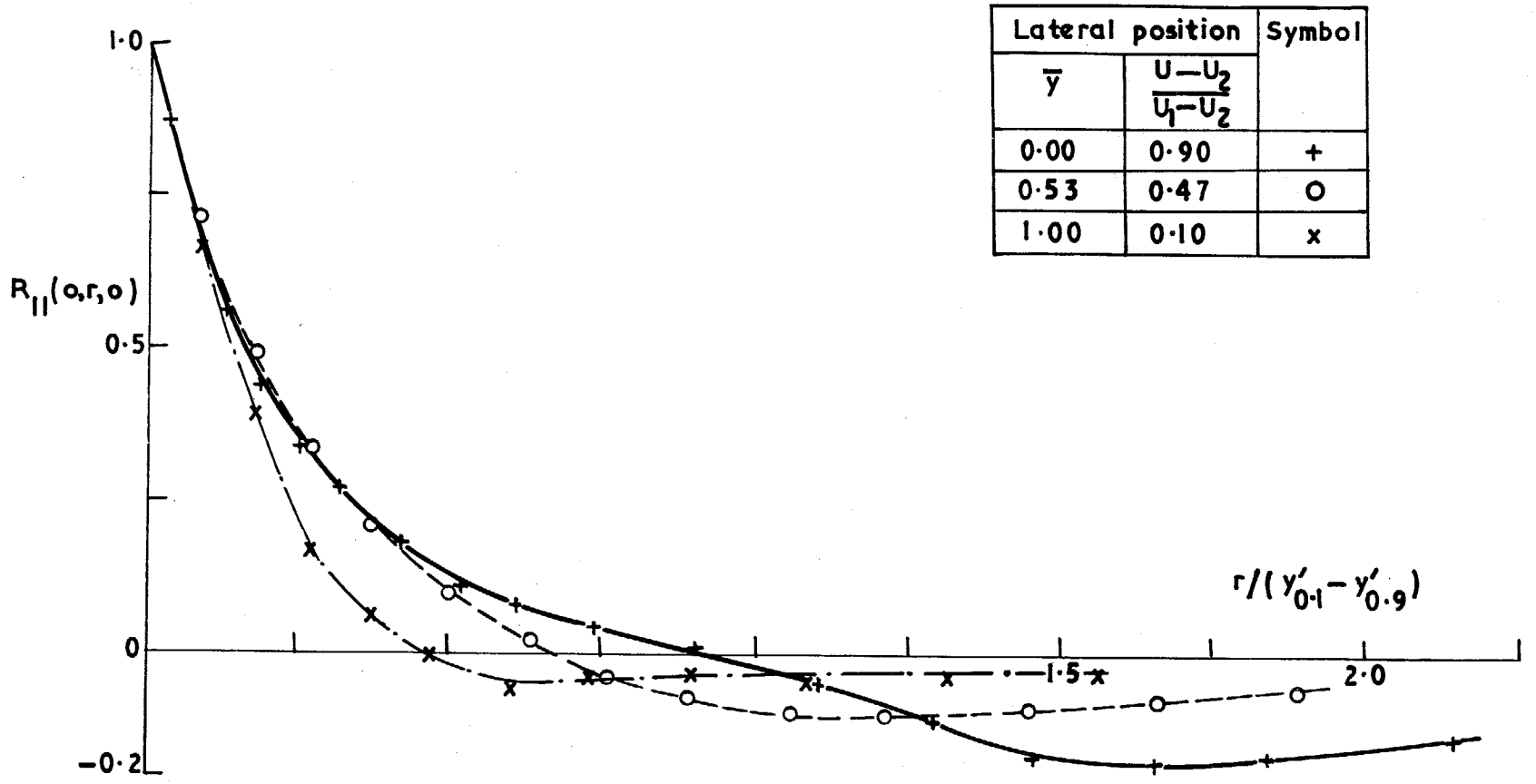


FIG. 17. Lateral correlation coefficient, $U_2/U_1 = 0{\cdot}61$, $x = 0{\cdot}67$ m.

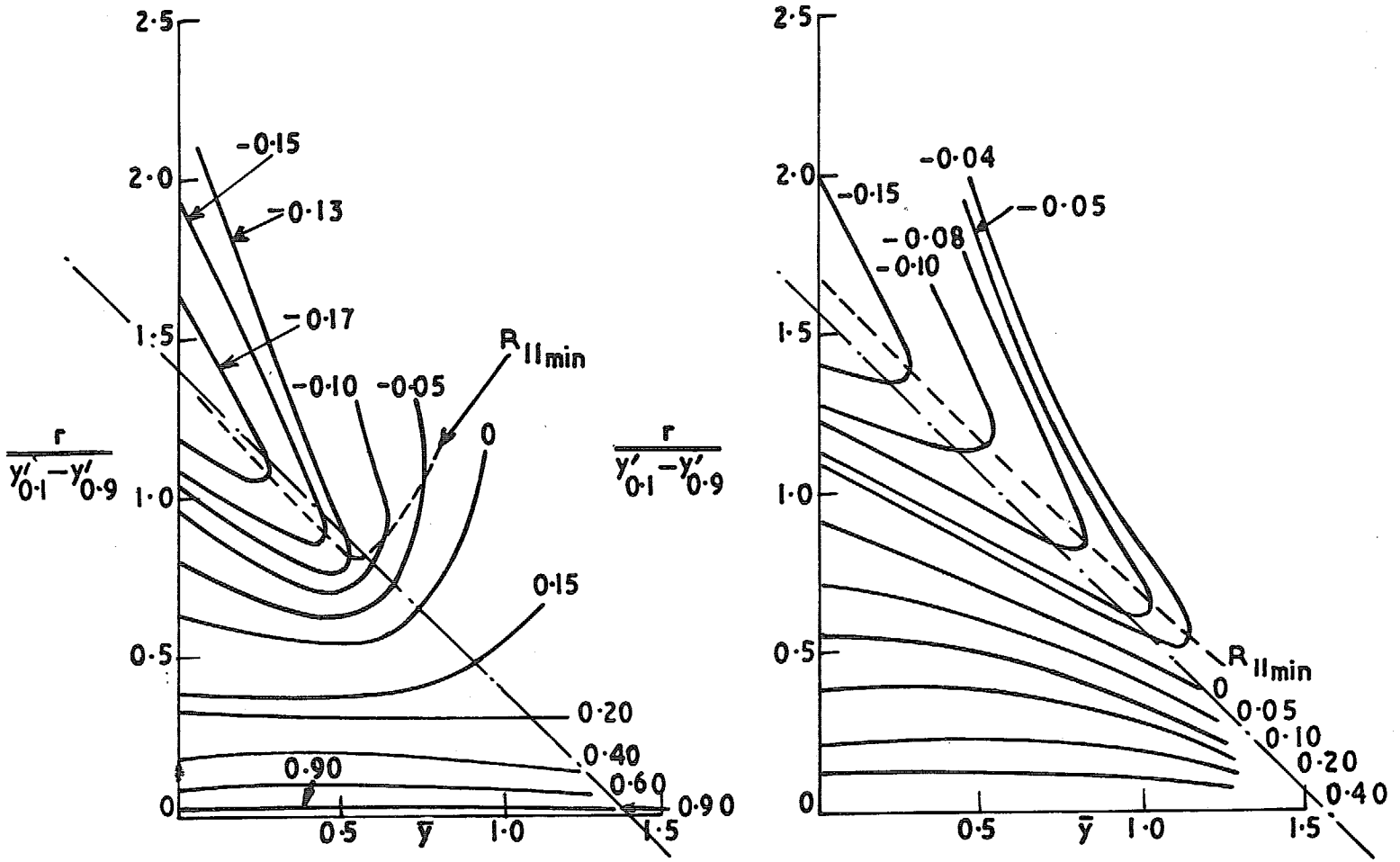


FIGS. 18 & 19. Contours of $R_{11}$ $(o, r, o)$, $U_2/U_1 = 0{\cdot}30$ & $0{\cdot}61$ respectively.

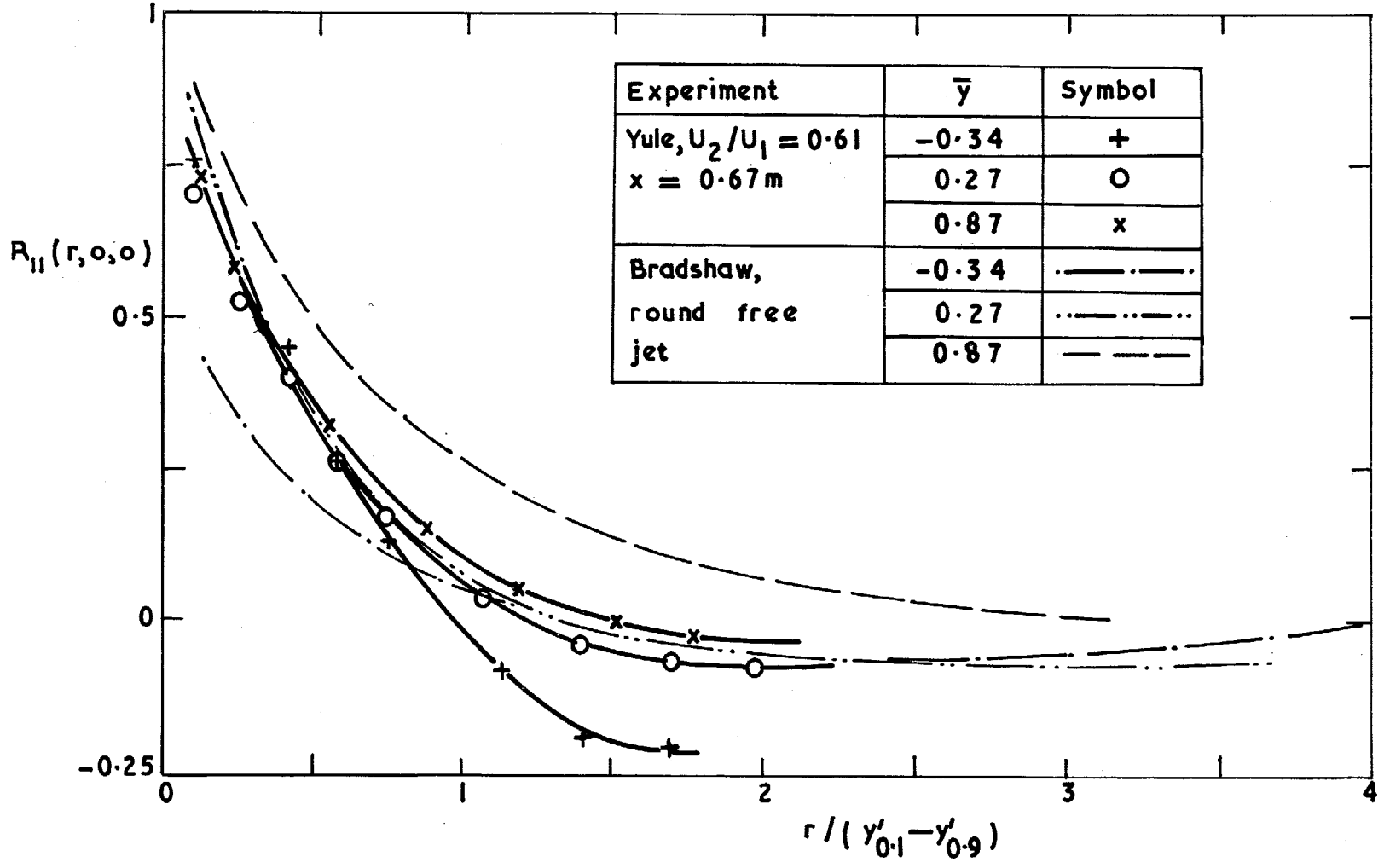


FIG. 20. Longitudinal correlation coefficient in mixing layers.

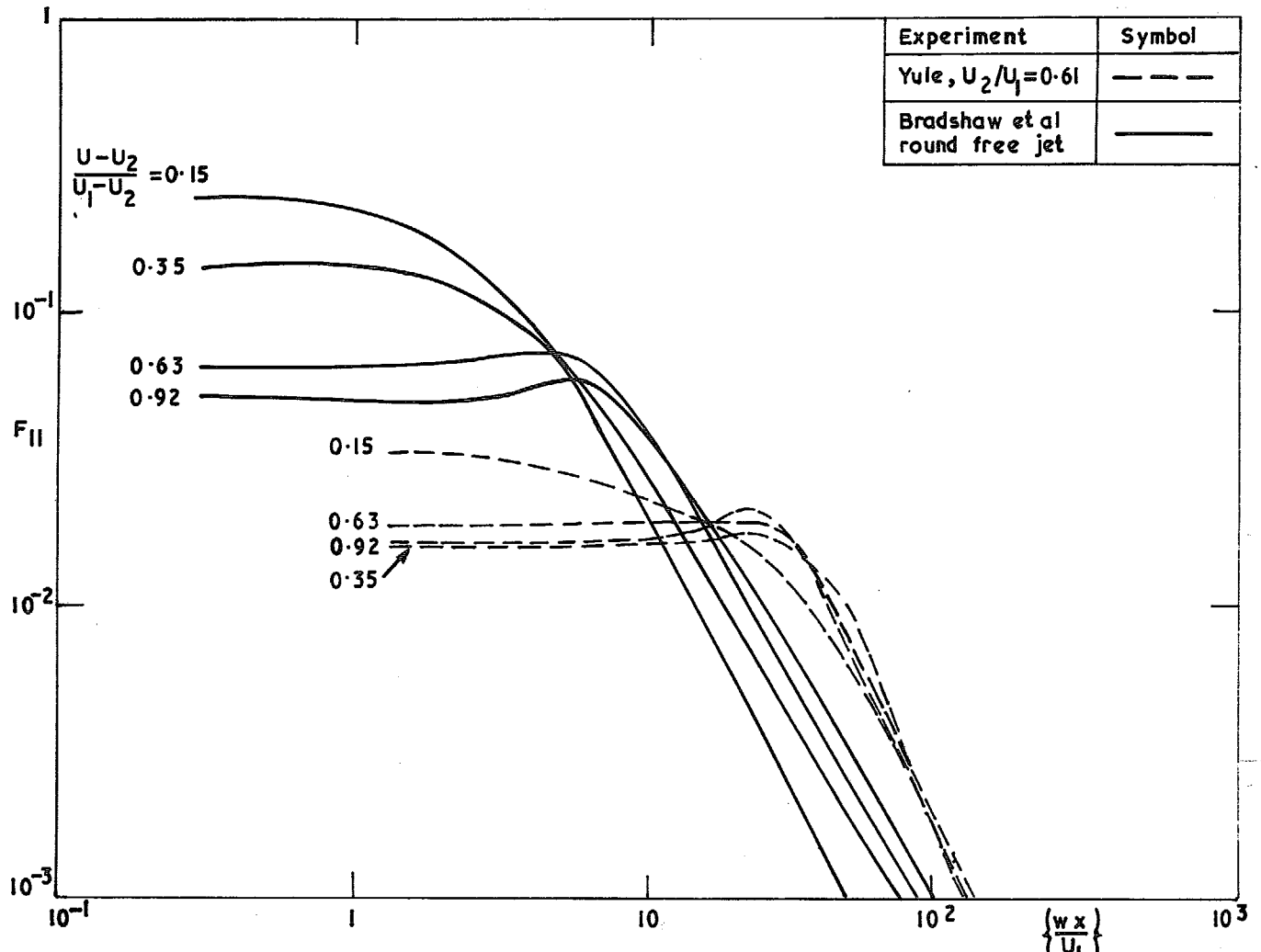


FIG. 21. Frequency spectra of $\overline{u^2}$ in mixing layers.

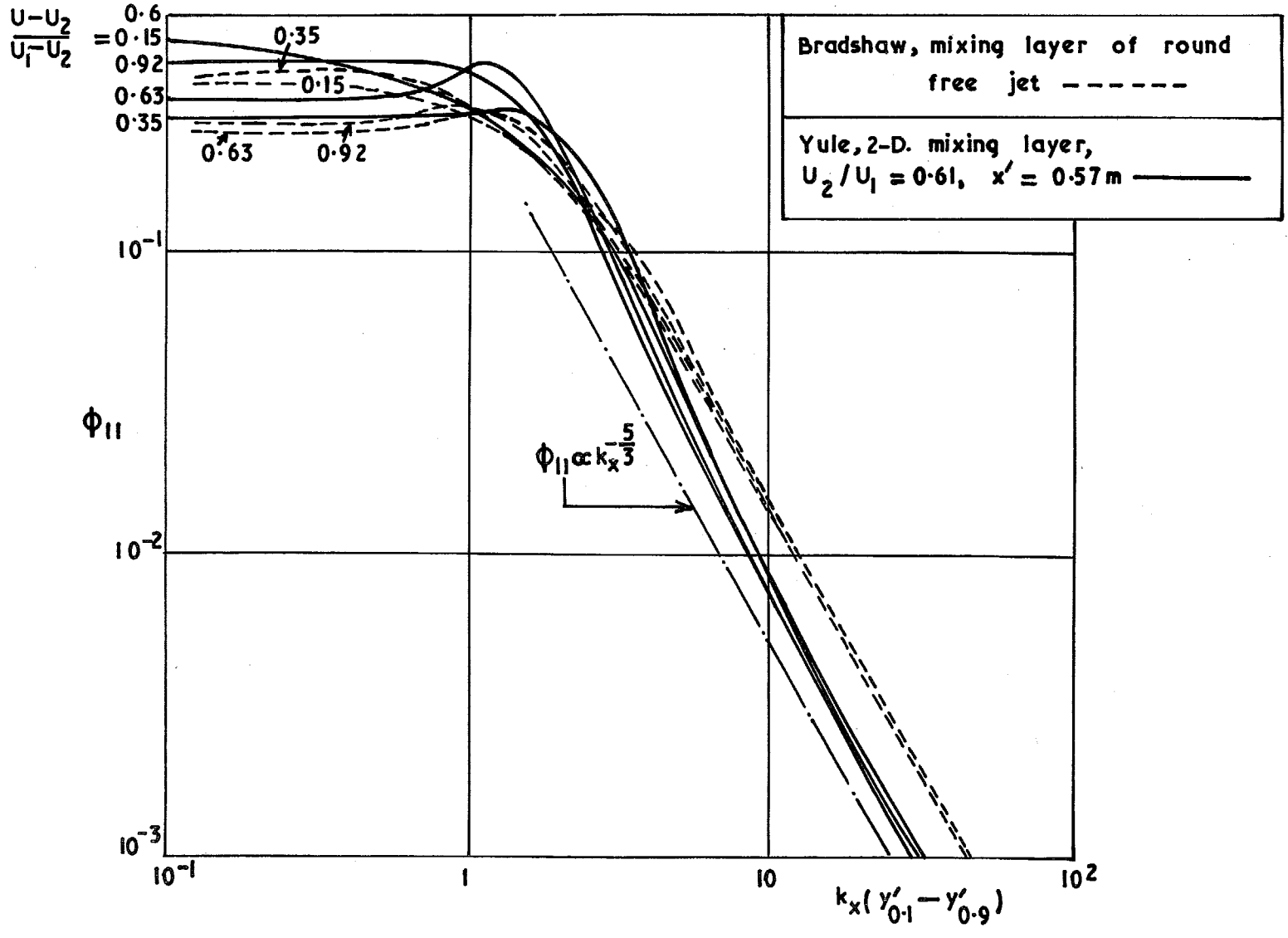


FIG. 22. One-dimensional wave number spectra.

Printed in Wales for Her Majesty's Stationery Office by Allens Printers (Wales) Limited.
Dd. 502110 K.5. 11/71

Published by
HER MAJESTY'S STATIONERY OFFICE

To be purchased from
49 High Holborn, London WC1V 6HB
13a Castle Street, Edinburgh EH2 3AR
109 St. Mary Street, Cardiff CF1 1JW
Brazennose Street, Manchester M60 8AS
50 Fairfax Street, Bristol BS1 3DE
258 Broad Street, Birmingham B1 2HE
80 Chichester Street, Belfast BT1 4JY
or through booksellers

R. & M. No. 3683

SBN 11 470483 X